INSTITUT DE CHIMIE
SEPARATIVE DE MARCOULE

New insights in the description of the dissolution of actinide dioxides : better understanding for their reprocessing

N. DACHEUX

ICSM, CEA, CNRS, ENSCM, Univ Montpellier, Bagnols sur Cèze, France

Transverse approach of the material elaboration

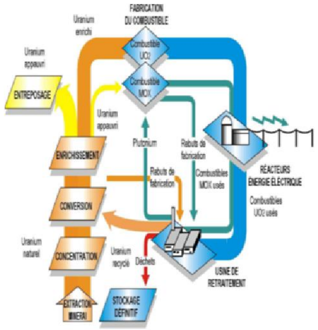

Sintering :
densification
microstructure

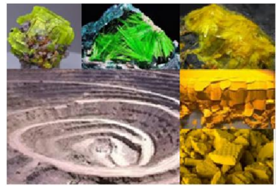

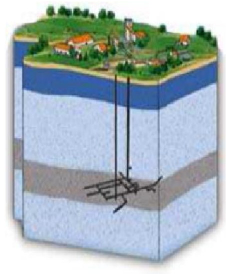

Dissolution

Leaching

Optimized Syntheses

Model compounds :
New ways of synthesis
New precursors

Properties in use :
Chemical durability
Long-term behavior

✦ Dissolution of AnO_2, $(An,Ln)O_{2-x}$ / Fluorite-type prepared by wet chemistry routes

- ❖ Conventional parameters (chemical composition, temperature, acidity, …)
- ❖ Structural parameters (oxygen vacancies, superstructure, secondary phases, …)
- ❖ Microstructural parameters (crystal defects, crystallite size, densification rate, …)

Distribution of FP and An in SNF

Spent Nuclear Fuel → U (95 wt.%) – Pu (1 wt.%) MA (0.1 wt.%) – FP (4 wt.%) → More than 40 FP 4 main types

PGM
(Ru, Rh, Pd)
≈ 0.6 mol.%

Lanthanides
(La, Ce, Pr, Nd)
≈ 1 mol.%

Actinides
(Np, Pu, Am, Cm)
≈ 1.1 mol.%

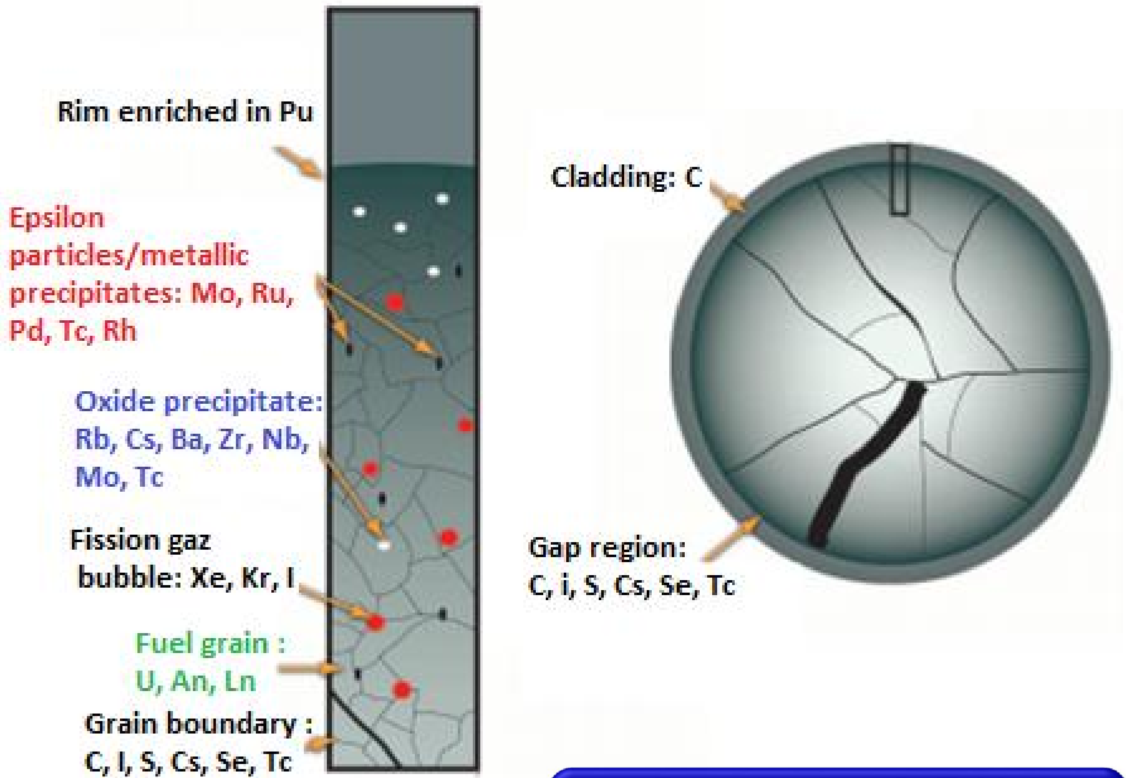

Which impact on UO_2 dissolution ?

P. Burns, R.C. Ewing, A. Navrotsky, *Science* 2012, 335, 1184-1187
PRECCI Report, CEA, 2001, CEA-R-5958E

Dissolution : a key step in the front-end of reprocessing

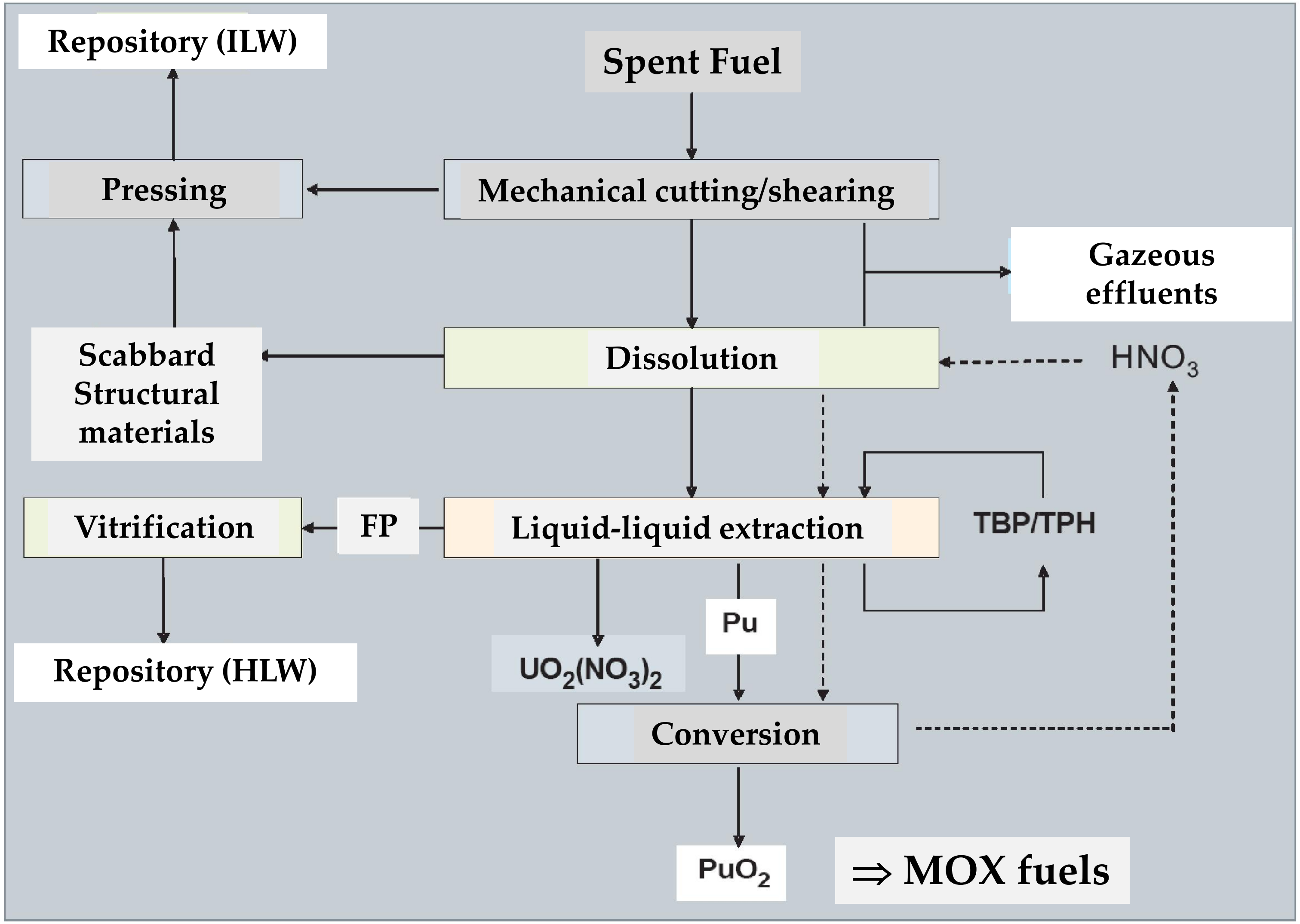

Monographie CEA, Ed. Le Moniteur,, 2008

Dissolution : a key step in the front-end of reprocessing

➢ *Shearing of the fuel pens*

Zircaloy scabbard / irradiated UO_2

➢ *Dissolution*

- **Hot and Concentrated HNO_3**
- **Oxidation of U(IV) into U(VI)**
- **Uptake of scabbards pieces with the help of bucket-wheel**

  ⇒ Specific conditioning

Necessity to better discriminate and prioritize the reactions and parameters driving dissolution: chemistry, radiolysis, structure, homogeneity, microstructure, …

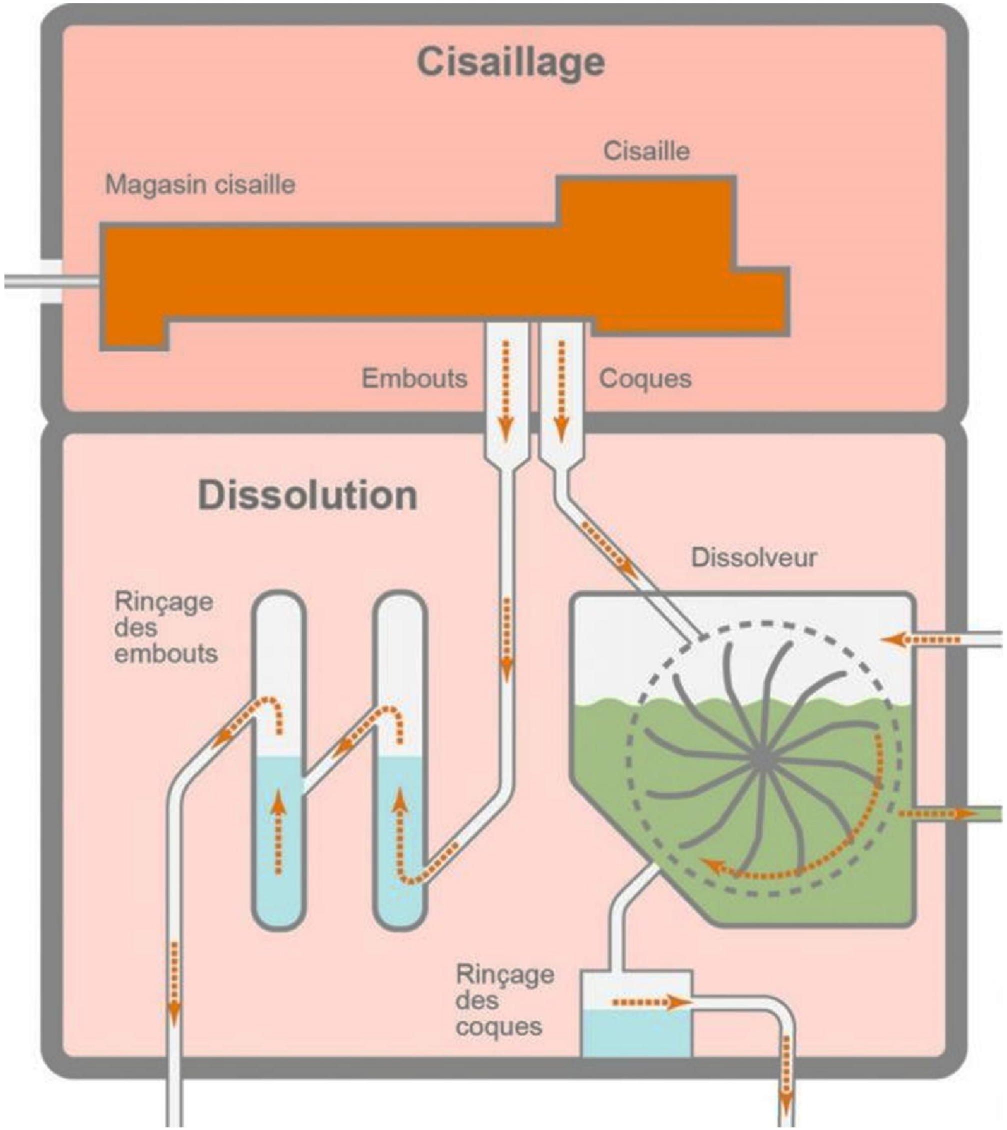

Methodology

Structural and microstructural control of starting materials

Model compounds

Synthesis / Densification

Impact of dissolving solution : pH, T, redox, composition…

$$R_L = k_0 \times e^{-E_A/RT} \times a(H_3O^+)^n \times g(I) \times \Pi\, a(i)^{n_i} \times f(\Delta_R G\,(\xi,T))$$

Dissolution experiments

Macroscopic dissolution rates

Macroscopic description of the dissolution

Microscopic description of the evolving interface

Monitoring of solid/liquid interface

Evolving structural and microstructural parameters

***Operando* analysis (ESEM, X-EDS, G-XRD, XRR, AFM)**

↳ Topography, porosity, chemical composition of interface

Preparation of model samples :
Powdered – Sintered
Actinide bearing oxides

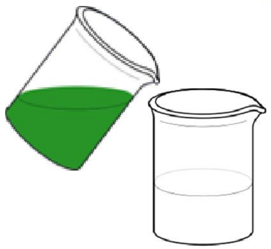

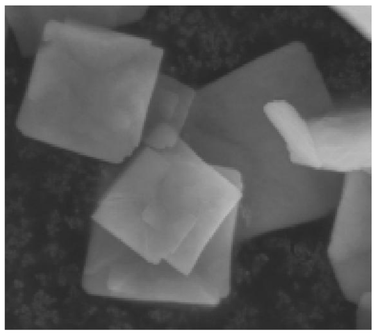

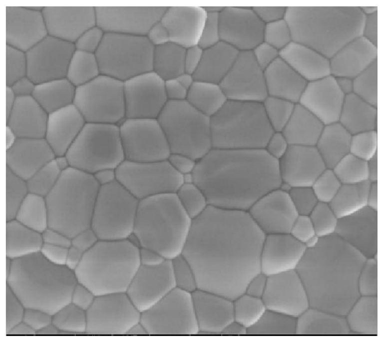

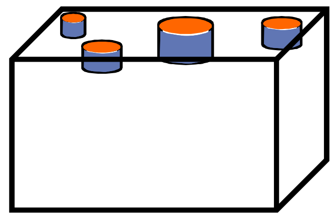

Preparation of $U_{1-x}Th_xO_2$ and $U_{1-x}Ln_xO_{2-x/2}$

Oxalate precipitation

Conversion

$Th_{1-x}U_x(C_2O_4)_2 \cdot 2\ H_2O$ (x = 0 – 1)

$U_{1-x}Ln_x(C_2O_4)_{2-x/2} \cdot n\ H_2O$ (x = 0.1 & 0.2)

↳ 7% Y – 13% La – 26% Ce – 12% Pr – 42% Nd

R. T.
$H_2C_2O_4$: + 50%

Washing
(H_2O – EtOH)

Drying
(90°C)

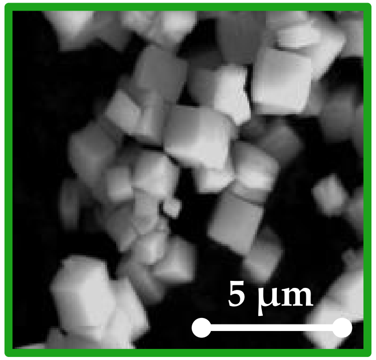

500°C / 4 h

Air
then
Ar / H_2

$Th_{1-x}U_xO_2$

$U_{1-x}Ln_xO_{2-x/2}$

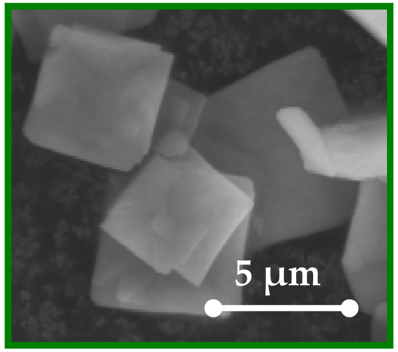

Platelet grains
≈ 5 µm in size

Quantitative precipitation for U and Th precipitation

	Expected mole ratio	Obtained (Dissolution)	Recovery yield (%)
U	0.9	0.89 ± 0.04	99.3 ✓
Ln(III)	0.1	0.11 ± 0.02	

Full dissolution ICP-AES

Y	0.07	0.06 ± 0.02	99.9 ✓
La	0.13	0.14 ± 0.03	93.8 ✓
Ce	0.26	0.31 ± 0.05	92.9 ✓
Pr	0.12	0.13 ± 0.08	98.7 ✓
Nd	0.42	0.42 ± 0.04	95.6 ✓

Characterization by XRD

➢ Complete solid solution for $Th_{1-x}U_xO_2$, following the Vegard's law

UO_2 | **$U_{0.9}Ln_{0.1}O_{1.95}$** | **$U_{0.8}Ln_{0.2}O_{1.9}$**

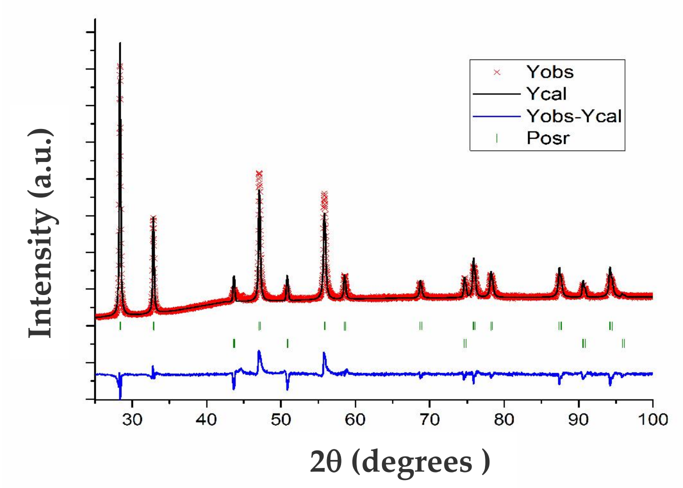

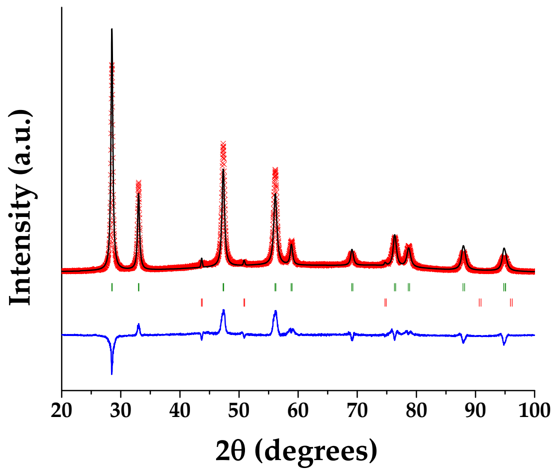

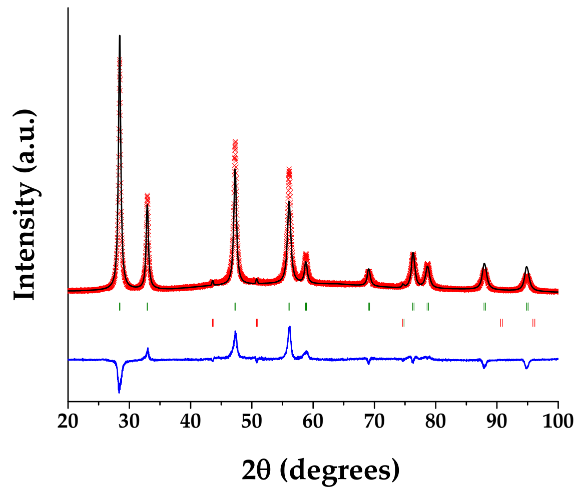

a = 5.466 Å → a = 5.442 Å → a = 5.438 Å

Literature :
a = 5.47127(8) Å

Incorporation of Ln(III) in the UO_2 Fluorite-type structure

G. Leinders, *J. Nucl. Mater.*, 2015, 459, 135-142

Sintering of $U_{1-x}Ln_xO_{2-x/2}$ samples

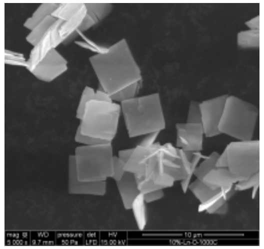

Grinding step
30 Hz / 30 min

Uniaxial pressing
RT – 500 MPa

Heating treatment
1550°C / 8h
Ar – 5% H_2

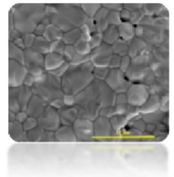

Characterization
PXRD, BET, ESEM, Pycnometry

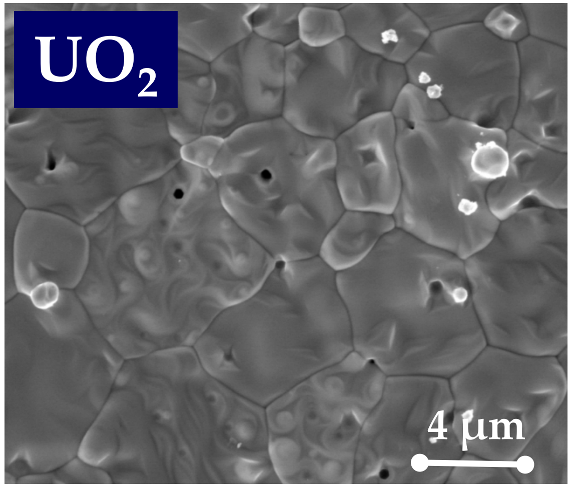

Densification rate: 93%
Average grain size: 11.8 µm

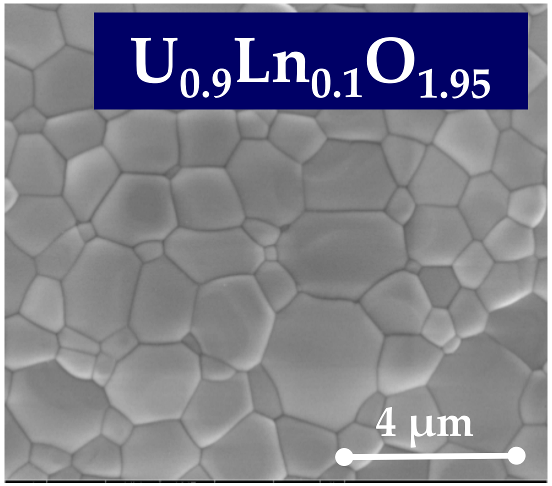

Densification rate: 90%
Average grain size: 3.4 µm

$U_{0.8}Ln_{0.2}O_{1.9}$

Densification rate: 87%
Average grain size: 0.9 µm

T. Cordara, *PhD*, University of Montpellier, 2017

Preparation of PGM doped UO_2

Hydroxide precipitation

UO_2 doped with 3% PGM
Rh (10%) – Ru (55%) – Pd (35%)

Room temperature
Excess of NH_4OH

U(IV) + PGM
HCl

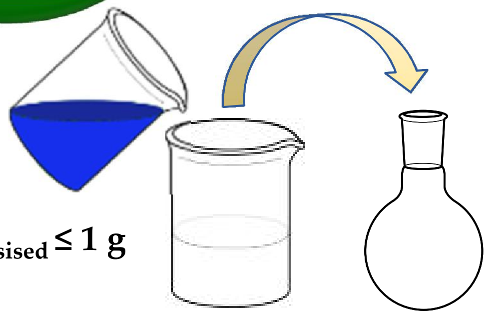

$m_{synthesised} \leq 1$ g

Washing
(water + ethanol)

Precipitate
+
EtOH

Drying under vacuum
T = 40°C

Recovery yield

- ☺ U : 99.9 %
- ☺ Ru : 90 %
- ☺ Pd : 100 %
- ☺ Rh : 85 %

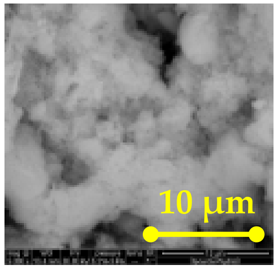

Highly reactive

120 – 150 $m^2.g^{-1}$

Crystallite size: 2-5 nm

800°C / 4 h

Ar / H_2

Conversion

a = 5.470 Å

a = 5.47127(8) Å (UO_2)*

Crystallite size: 130 nm

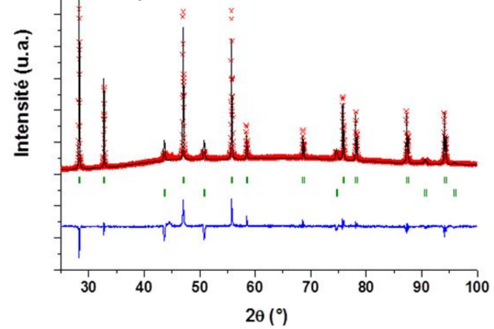

No PGM in the UO_2 structure

J. Martinez, *Patent FR3016360 – WO2015/107086, 2015*
N. Clavier *et al.*, *Chem. Phys. Chem.*, 2017, 18, 2666-2674
T. Cordara, *J. Nucl. Mater.*, 2019, Submitted
* G. Leinders, *J. Nucl. Mater.*, 2015, 459, 135-142

Sintering of UO_2 : PGM

Uniaxial pressing
RT – 500 MPa

Heating treatment
1550°C / 8h
Ar – 5% H_2

Characterization
PXRD, BET, ESEM,
Pycnometry

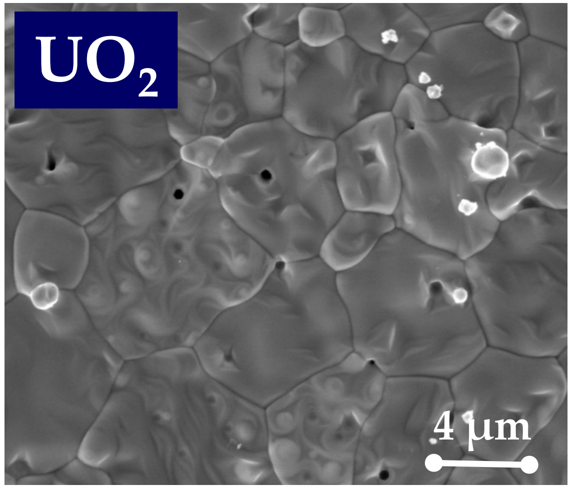

Densification rate: 93%
Average grain size: 11.8 µm

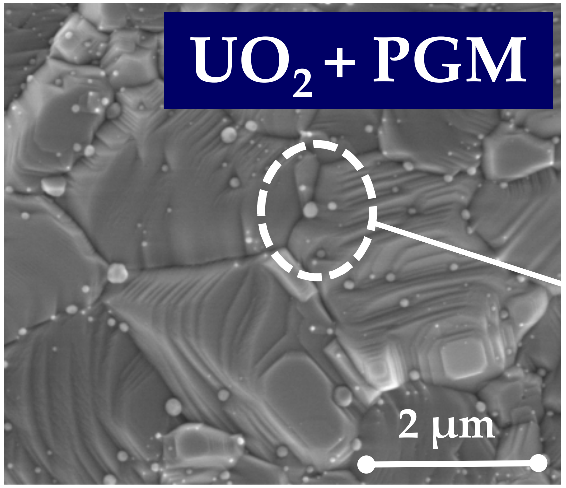

Densification rate : 89%
PGM-aggregates < 0.5 µm
UO_2 grains size ≈ 1-5 µm

Ru, Rh, Pd bearing aggregates located at GB (surface + inner)

SNF

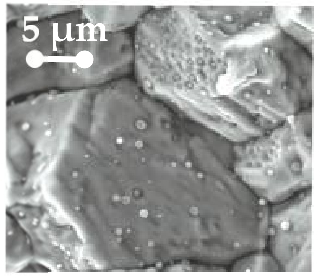

T. Cordara, *J. Nucl. Mater.*, 2019, Submitted
J. Noirot, *Monographie CEA*, 2009, 25-28

Chemical durability of the ceramics during dissolution processes

Dissolution test: experimental device

Powder, Pellet

Static conditions
Dynamic conditions

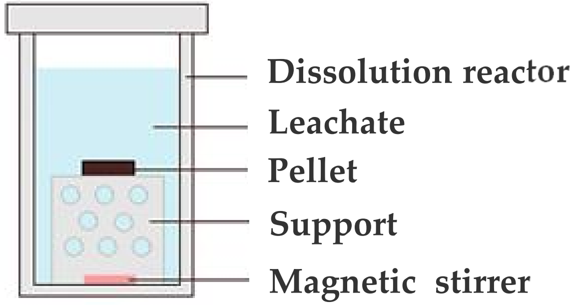

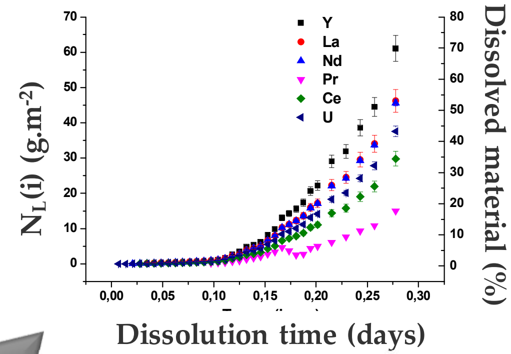

$$R_L(i) = \frac{d\,N_L(i)}{d\,t} = \frac{1}{f_i \times S} \times \frac{d\,m_i}{d\,t}$$

$$N_L(i) = \frac{m_i}{f_i \times S}$$

Amount of (i) in solution (g)

Reactive surface area (m²)

Mass ratio of (i) in the solid

	$R_{L,0}$ (i) (g.m^{-2}.d^{-1})	$R_{L,0}$ (U)/$R_{L,0}$ (Ln)
U	5,4 ± 0,2	--
Y	< L.Q.	--
La	7,8 ± 0,1	1,4
Pr	< L.Q.	--
Nd	6,8 ± 0,2	1,3
Ce	4,9 ± 0,2	0,9

ICP–AES
ICP-MS
α liquid scintillation

$R_L(i) \approx R_L(j)$: congruent dissolution
$R_L(i) \neq R_L(j)$: incongruent dissolution

Characterization of solution, solid and interface

❷ *Study of the surface (sub-surface) of the material*
Identification of the dissolution mechanisms

Techniques for observations :

- ✓ Optical microscopy, SEM, ESEM, TEM, …

Techniques for surface analysis :

- ✓ Grazing XRD, XRR, …
- ✓ Spectroscopy (UV, IR, Raman, TRLIFS, …)
- ✓ EPMA, EELS, X-EDS, …
- ✓ XPS, EXAFS, XANES, …

❖ **To determine :**

- ✓ Thickness of the altered layer
- ✓ Nature of the altered layer
- ✓ Characterization of neoformed phases

Analysis and quantification of elements released in solution ❶

Elementary concentration determination :

- ✓ Dissolved species, colloidal species
- ✓ Analytical techniques :
  ICP-MS, ICP-AES,
  α or β scintillation, α or β spectroscopy

Species distribution (speciation) :

- ✓ Redox, complexation, acid-base reactions

❖ **Access to :**

- ✓ Direct determination of C_{Mi}
- ✓ Evaluation of weight loss : Δm_{mat}
- ✓ Saturation indexes

Normalization tools :

$$N_L(i) = \frac{\Delta m_i}{x_i \times S}$$

$$R_L(i) = \frac{d\, N_L(i)}{dt} = \frac{1}{x_i \times S} \times \frac{d}{dt}(\Delta m_i)$$

Description of dissolution & saturation mechanisms

Schematic representation of ceramic dissolution

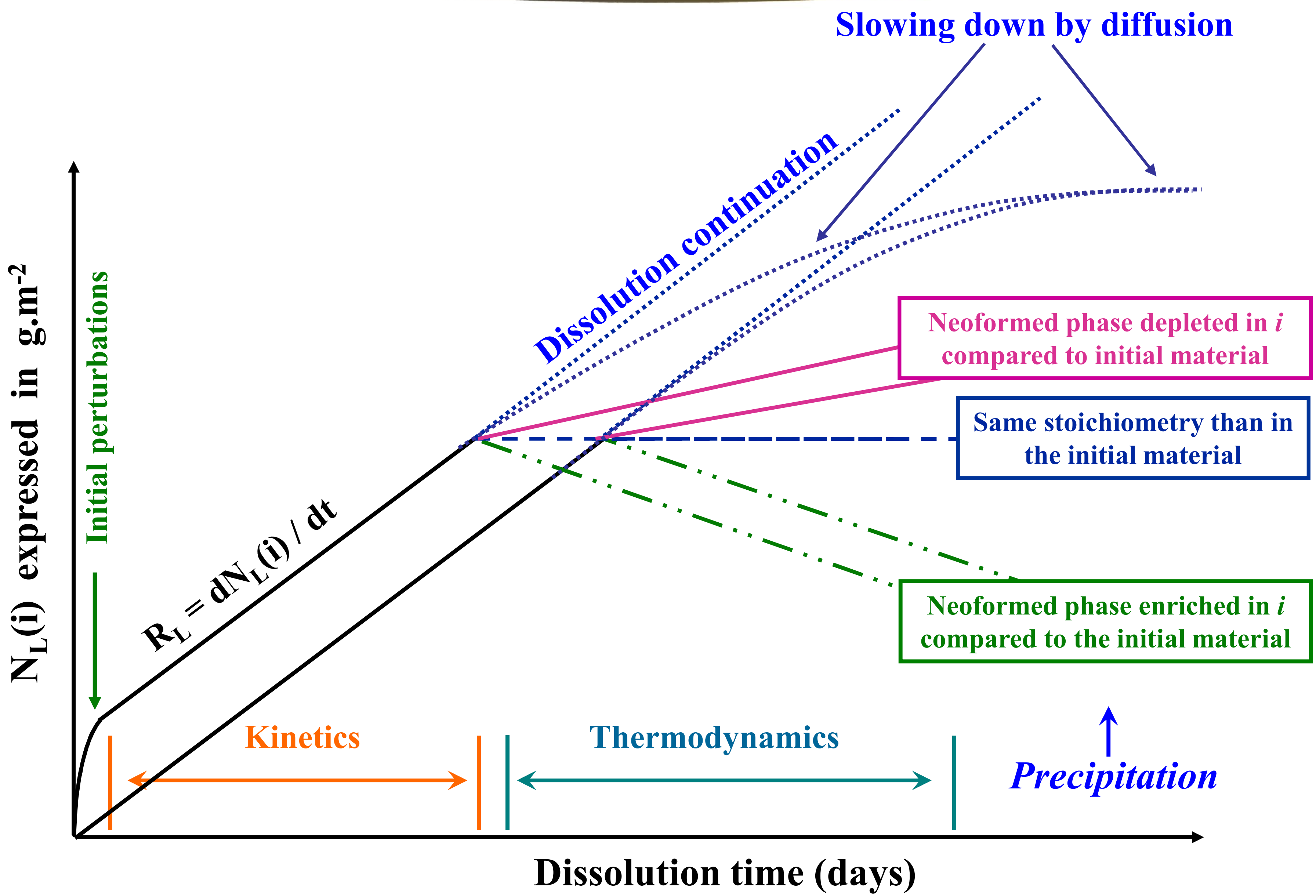

Macroscopic study

Multiparametric expression of the dissolution kinetics

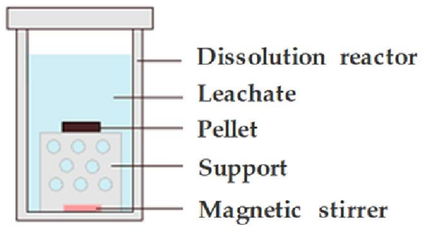

$$R_L = k_0 \times e^{-\frac{E_A}{RT}} \times (H_3O^+)^n \times g(I) \times (E_i)^{ni} \times f(\Delta_r G)$$

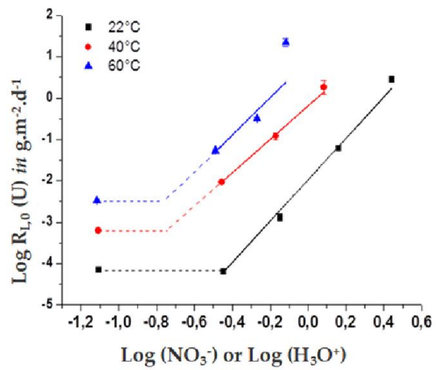

A.C. Lasaga, *Kinetic Theory in the Earth Sciences,* Princeton Univ. Press, 1998

Kinetics of materials (minerals) dissolution

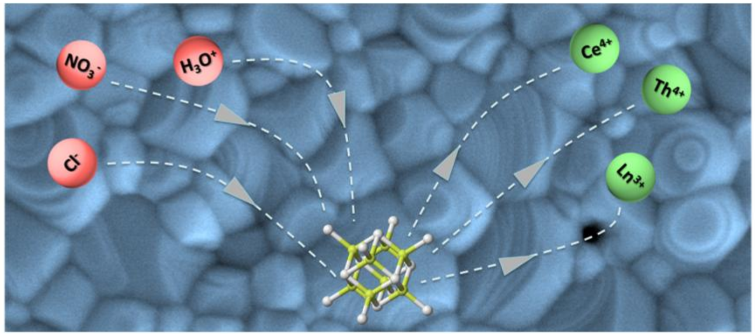

D. Horlait et al., J. Mater. Chem. A, 2 (2014) 5193

✦ A.C. Lasaga : Geochemical approach

⇒ Activated Complex Theory

- Only chemical effects (solution)
- Control more often by surface reactions
- No microstructural effect (solid)

$$R_L = k_0 \times e^{-E_A/RT} \times a_{H+}^{\ n} \times g(I) \times \prod a_i^{mi} \times f(\Delta_R G)$$

- Temperature contribution
- Acidity contribution
- Ionic strength contribution
- Redox, complexing contributions
- Deviation from thermodynamic equilibrium

A.C. Lasaga et al., Rev. Mineral., 31 (1995) 23
A.C. Lasaga et al., J. Geophys. Res., 89 (1984) 4009

Impact of conventional parameters (acidity, temperature, …) on the dissolution kinetics

General trend of UO_2 dissolution in nitric acid

Kinetics
3 domains

- $R_{L.pulse}$ (U)
- $R_{L.0}$ (U)
- $R_{L.t}$ (U)

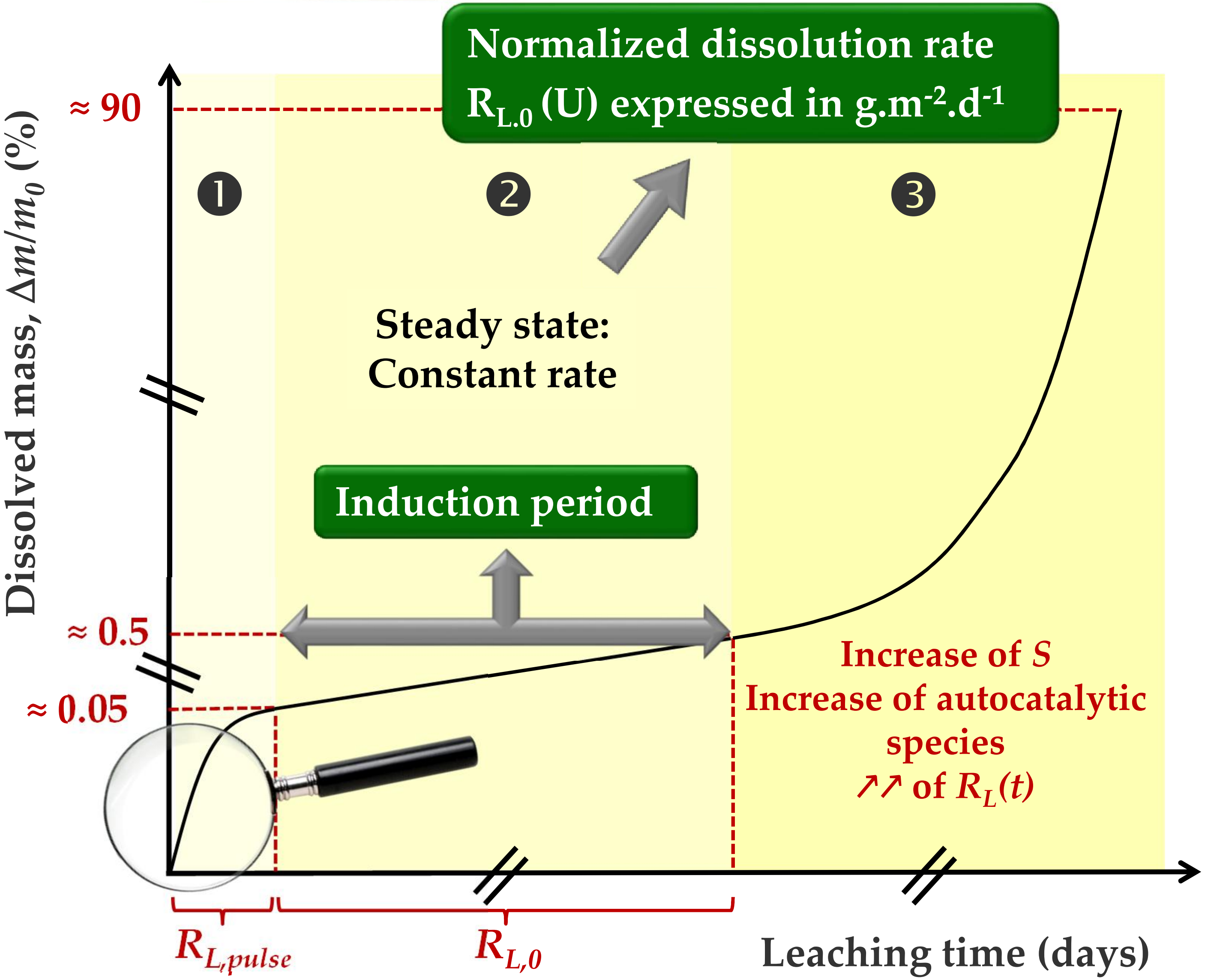

T. Cordara *et al.*, *J. Nucl. Mater.* 2017, 496, 251-264
T. Dalger *et al.*, *J. Nucl. Mater.* 2018, 510, 109-122

Impact of temperature on UO_2 dissolution

Reference
Sintered UO_2

0.1 – 0.5 – 1 – 2M HNO_3
T : 22°C – 40°C – 60°C
Static conditions

$$R_L = k \times e^{-\frac{E_A}{RT}}$$

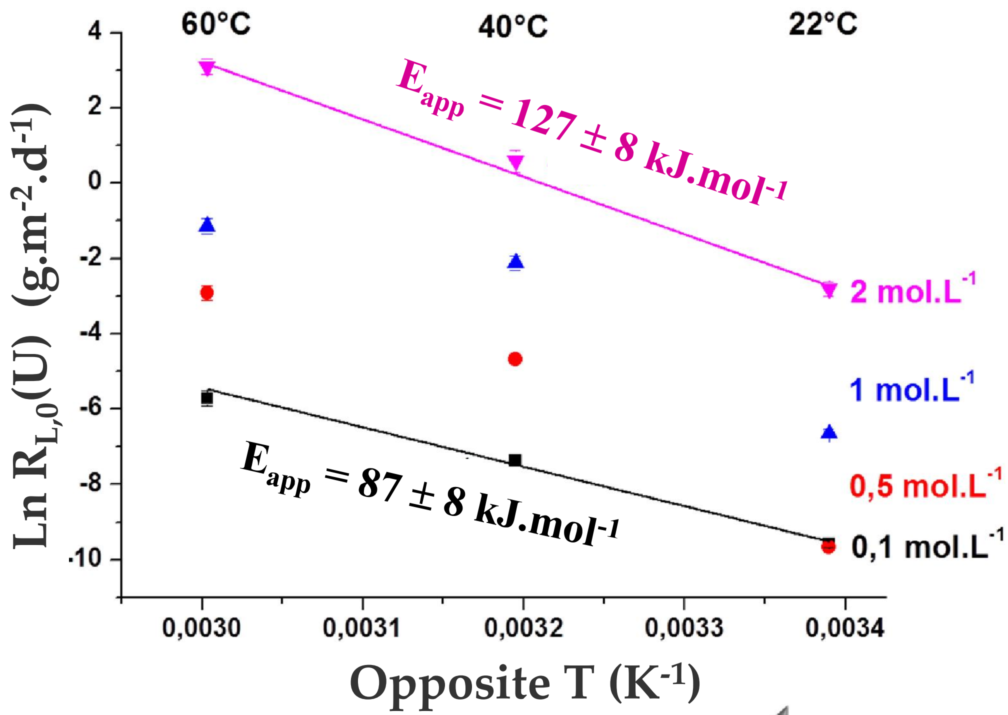

Impact of the acid concentration on the activation energy due to change in predominant mechanism: Surface controlling ⇒ Redox controlling reactions

Impact of acid concentration on UO_2 dissolution

Reference Sintered UO_2

0.1 – 0.5 – 1 – 2M – 4M HNO_3
T : 22°C – 40°C – 60°C
Static conditions

$R_L = k_T' \times (H_3O^+)^n$

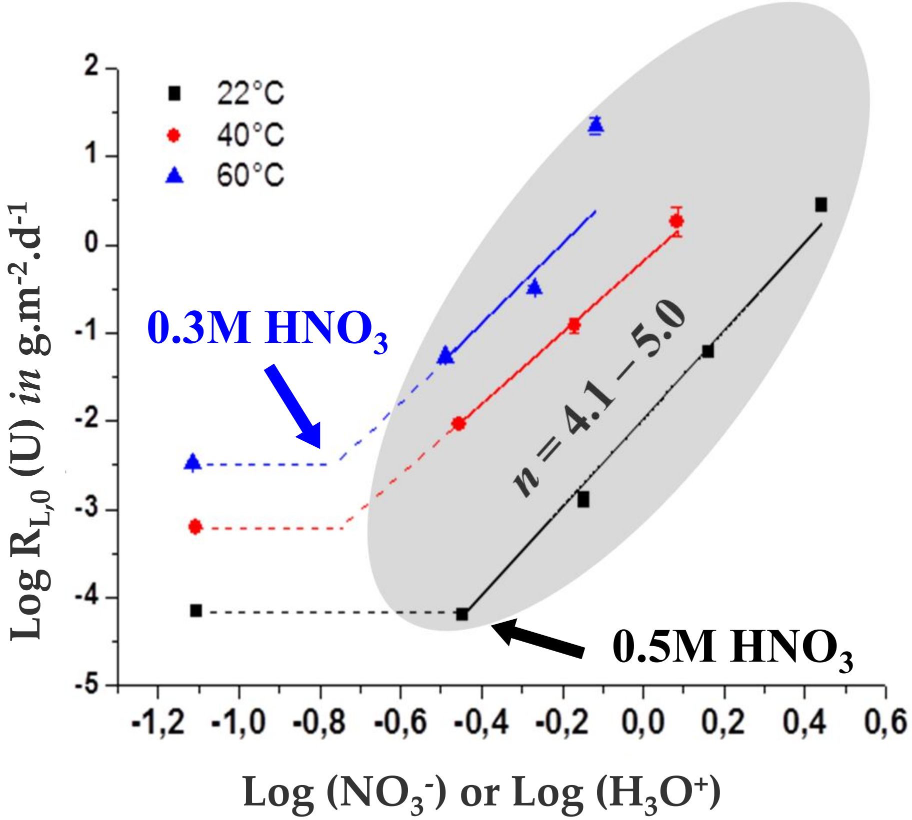

Modification of the <u>preponderant</u> dissolution mechanism with acid concentration

$C_{HNO3} < 0.5$ M $\Rightarrow$ Surface controlling reactions
$C_{HNO3} > 0.5$ M $\Rightarrow$ Redox controlling reactions

Dissolution of $Th_{1-x}U_xO_2$ solid solutions

Composition

2M HNO_3, T = 60°C
Static conditions

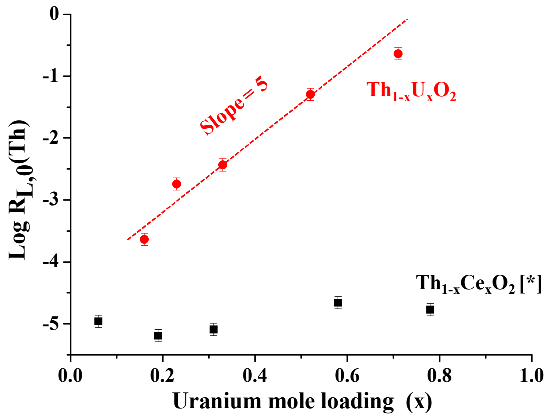

Acidity

$R_L = k_T' \times (H_3O^+)^n$

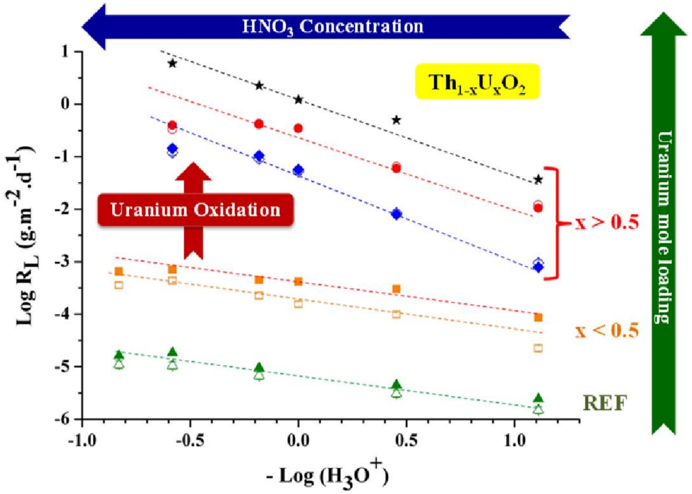

Temperature

$$R_L = k \times e^{-\frac{E_A}{RT}}$$

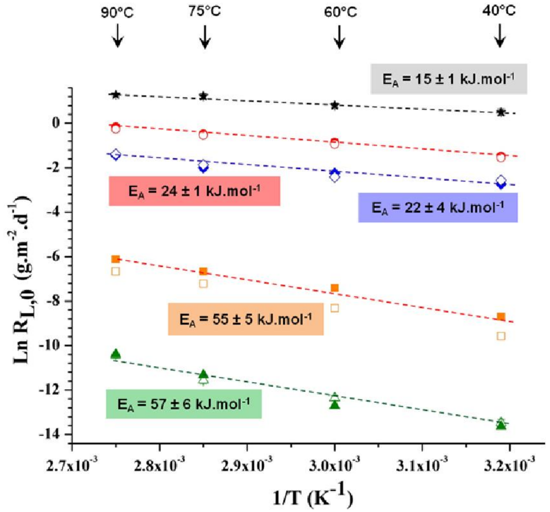

Strong increase of R_L(i) with the amount of U

Oxidative process
U(IV) → U(VI)

Modification of the controlling dissolution mechanism with U mole fraction ($x_U > 0.5$)

x < 0.5 ⇒ Surface controlling reactions
x > 0.5 ⇒ Redox controlling reactions

L. Claparede *et al.*, *J. Nucl. Mater.*, 2015, 457, 304-316

J. De Pablo *et al.*, *Geochim Cosmochim Acta*, 1999, 63, 3097-3103

Impact of HNO_2 on dissolution

$U_{0.75}Th_{0.25}O_2$

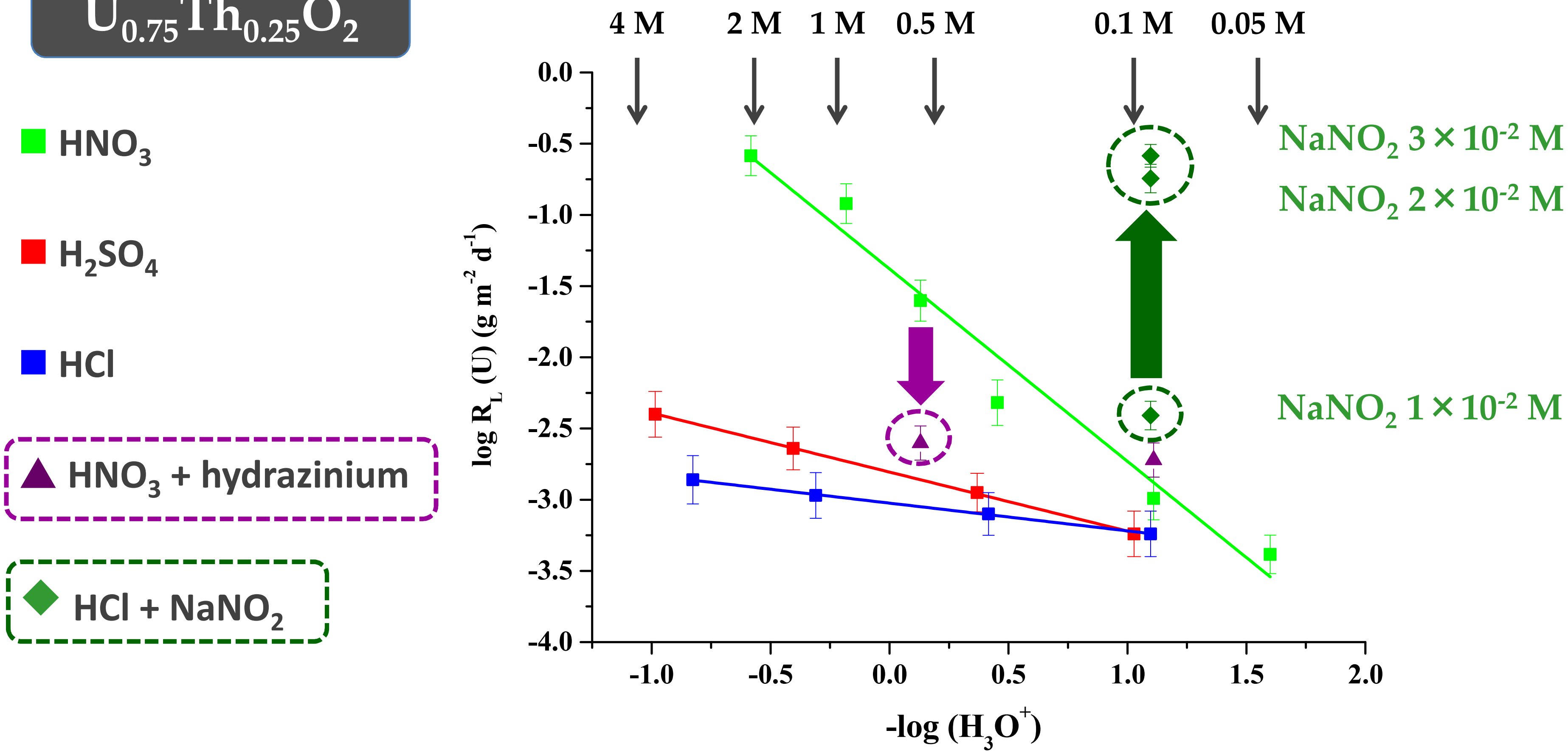

Strong increase of the dissolution rate with HNO_2
Lower impact of H_3O^+ et NO_3^-

F. Tocino, PhD, ICSM/CEA, Univ. Montpellier, Dec. 2015
T. Dalger, PhD, ICSM/CEA, Univ. Montpellier, 2016–2019

T. Dalger *et al.*, *J. Nucl. Mater.* 2018, 510, 109-122

Dissolution of $U_{1-x}Ln_xO_{2-x/2}$ solid solutions

$U_{0.9}Ln_{0.1}O_{1.95}$

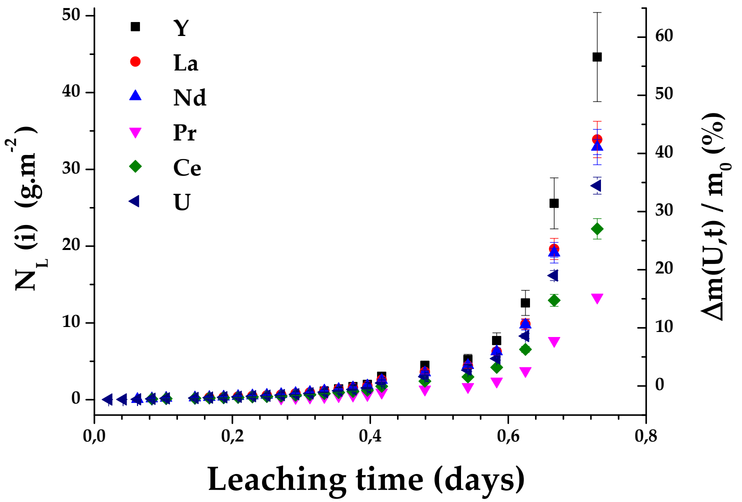

$U_{0.8}Ln_{0.2}O_{1.9}$

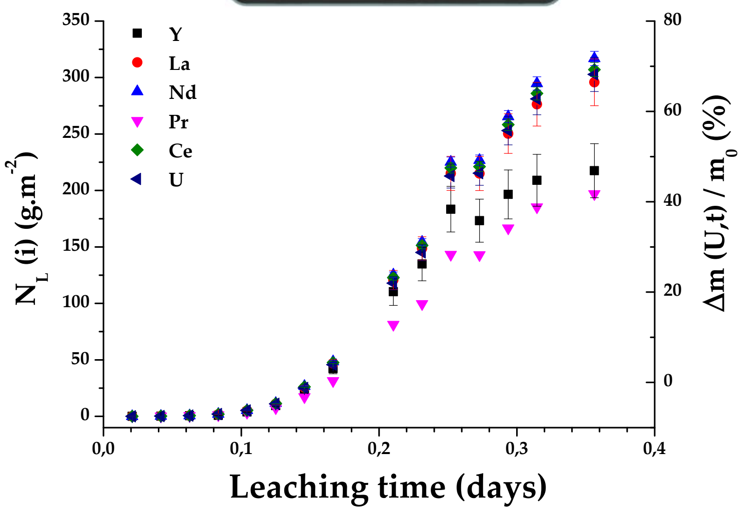

Congruent dissolution Ln(III) / U
In agreement with other systems (Th- & Ce-based)

Strong impact of Ln(III) on $R_{L,0}$ for low acicity (C_{HNO3} < 1M)
e.g. increase by a factor up to ≈ 20 for $U_{0.9}Ln_{0.1}O_{1.95}$ *vs.* UO_2
Small impact for higher acid concentrations (C_{HNO3} > 2M)

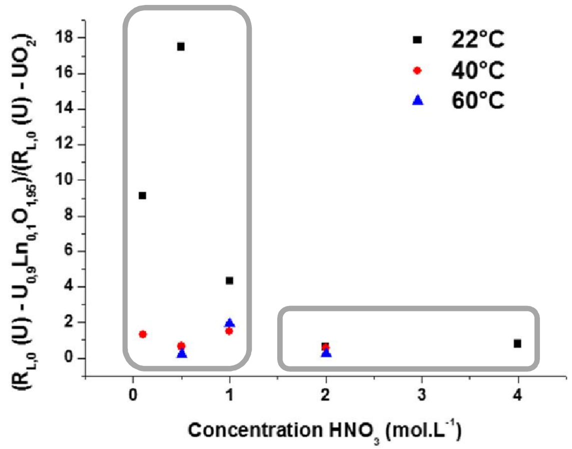

D. Horlait et al., *J. Mater. Chem. A*, 2014, 2, 5193 – *J. Nucl. Mater.*, 2012, 429, 237; S. Szenknect et al., *J. Phys. Chem. C*, 2012, 116, 12027

Dissolution of $U_{0.9}Ln_{0.1}O_{1.95}$ solid solution

Sintered $U_{0.9}Ln_{0.1}O_{1.95}$

0.1 – 0.5 – 1 – 2M – 4M HNO_3
T : 22°C – 40°C – 60°C
Static conditions

$$R_L = k \times e^{-\frac{E_A}{RT}}$$

+

$$R_L = k_T' \times (C_N)^{n'}$$

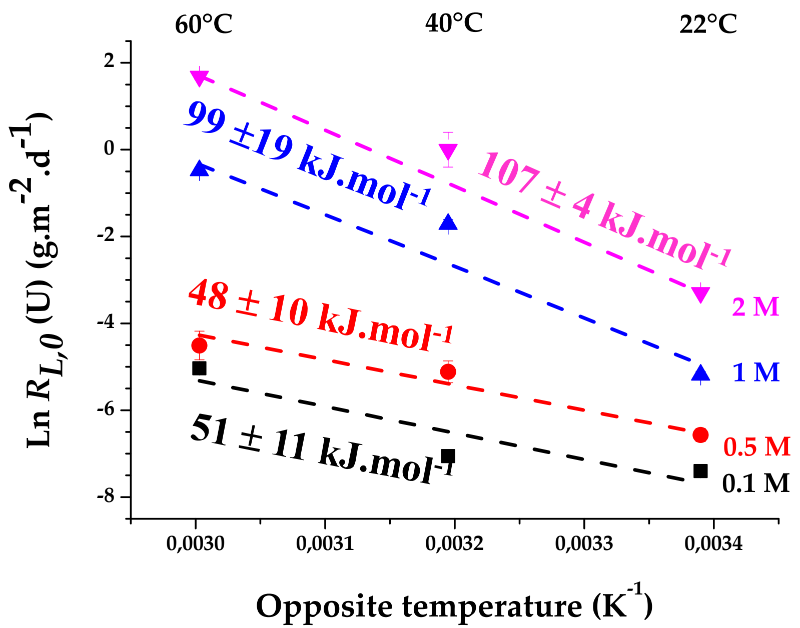

Modification of the preponderant dissolution mechanism with acid concentration

- $C_{HNO3} \leq 0.5$ M $\Rightarrow$ $E_{app} \approx 50$ kJ.mol^{-1} and n' fractional
  - ↳ Surface controlling reactions
- $C_{HNO3} > 0.5$ M $\Rightarrow$ $E_{app} \approx 100$ kJ.mol^{-1} and $n' > 2$
  - ↳ Redox controlling reactions

Dissolution of UO_2 doped with PGM

UO_2 doped with 3% PGM
Rh (10%) – Ru (55%) – Pd (35%)

0.1 – 0.5 – 1 – 2M – 4M HNO_3
T : 22°C – 40°C – 60°C
Static conditions

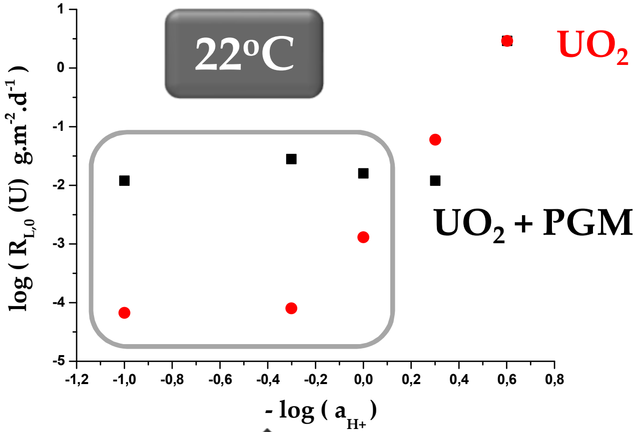

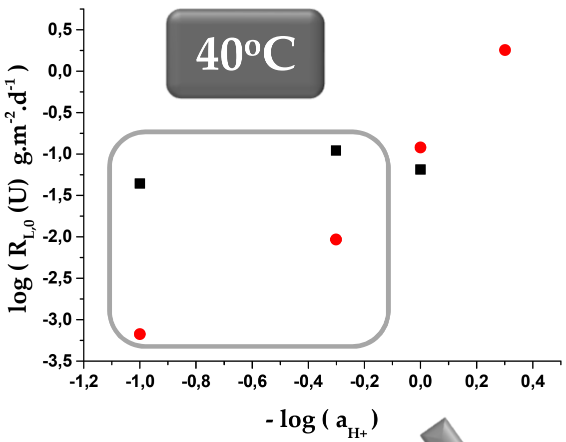

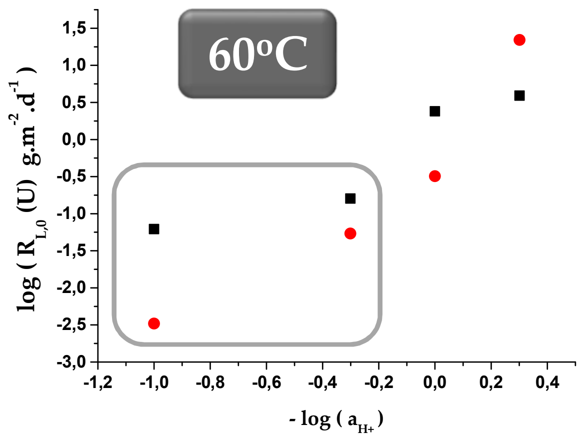

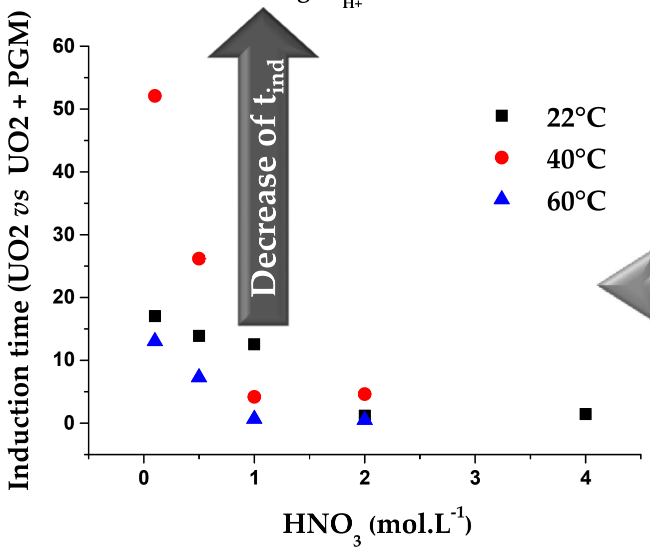

Very strong impact of PGM on $R_{L,0}$(U)
More important in less acidic media
Associated to reduction of induction period

T. Cordara, *J. Nucl. Mater.*, 2019, Submitted
T. Kaczmarek, *PhD*, Univ. Montpellier (2018-2021)

Dissolution of UO_2 doped with PGM

UO_2 doped with 3 mol% PGM
Rh (10%) – Ru (55%) – Pd (35%)

0.1 M HNO_3 – 22°C
Static conditions

UO_2 + PGM

$R_{L,0}$ (U) = (1.2 ± 0.2) × 10^{-2} g.m^{-2}.d^{-1}

UO_2

$R_{L,0}$ (U) = (6.7 ± 0.3) × 10^{-4} g.m^{-2}.d^{-1}

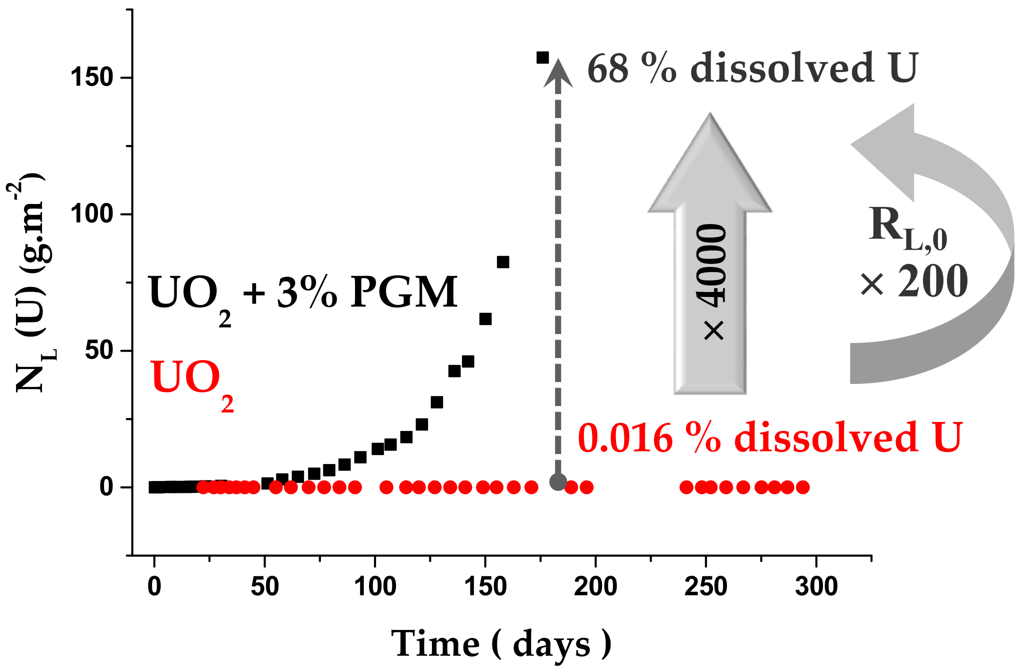

Strong impact associated to the presence of PGM on $R_{L,0}$(U)

- Solid contribution @ the solid/liquid interface ?
- Solution contribution: reduction of HNO_3 by PGM then production of autocatalytic species in solution (e.g. HNO_2) ?

Dissolution of UO_2 doped with PGM

UO_2 doped with 3 mol% PGM
Rh (10%) – Ru (55%) – Pd (35%)

0.1 M HNO_3
T : 22°C – 40°C – 60°C
Static conditions

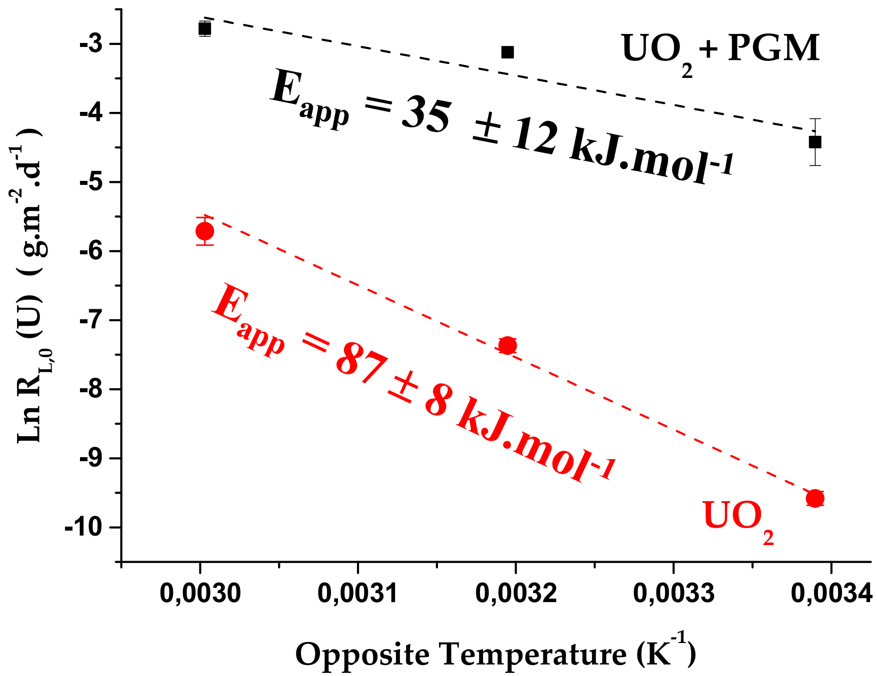

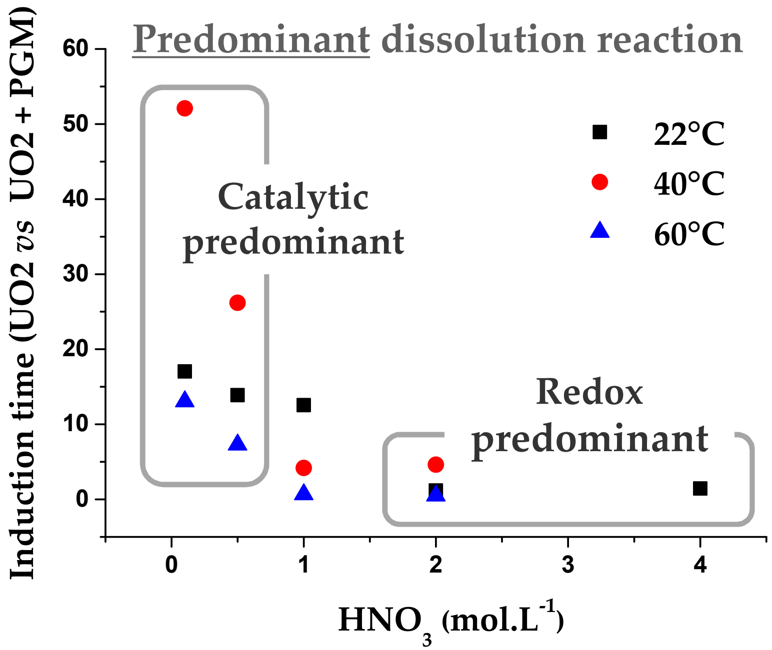

Significant decrease of E_A with PGM

Catalytic process
Predominant in less acidic media
Solution + at solid/liquid interface ?

Impact of PGM : contribution in solution

Sintered UO_2
+ PGM (in solution)

0.1 HNO_3 – 60°C
Static conditions

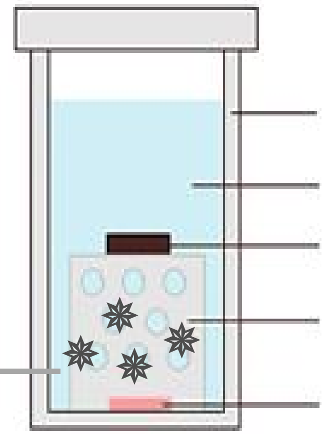

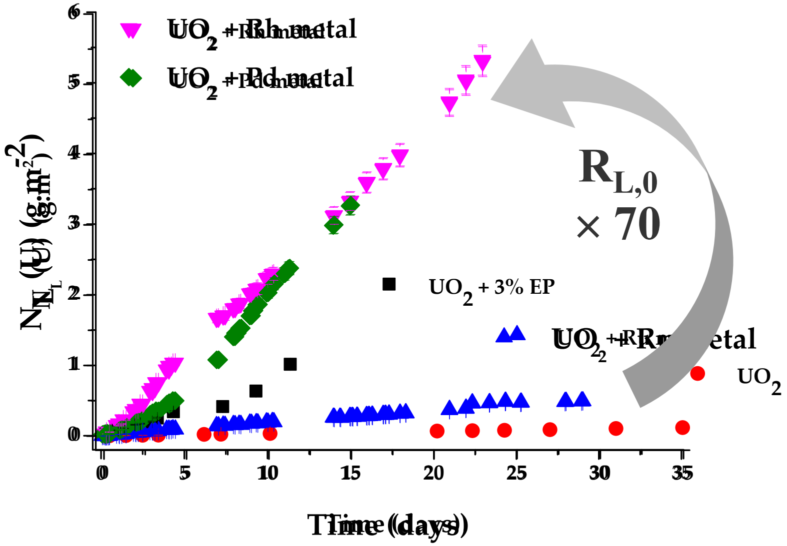

Rh: $R_{L,0}$ (U) = (2.3 ± 0.1) × 10^{-1} $g.m^{-2}.d^{-1}$
Pd: $R_{L,0}$ (U) = (9.3 ± 0.2) × 10^{-2} $g.m^{-2}.d^{-1}$
Ru: $R_{L,0}$ (U) = (1.8 ± 0.1) × 10^{-2} $g.m^{-2}.d^{-1}$

Pure UO_2
$R_{L,0}$ (U) = (3.3 ± 0.1) × 10^{-3} $g.m^{-2}.d^{-1}$

Increase of $R_{L,0}$ (U) in the presence of PGM powders → Catalytic effect associated to PGM <u>in solution</u>

Impact of microstructural parameters on the dissolution kinetics

Role of microstructural (hidden) parameters ?

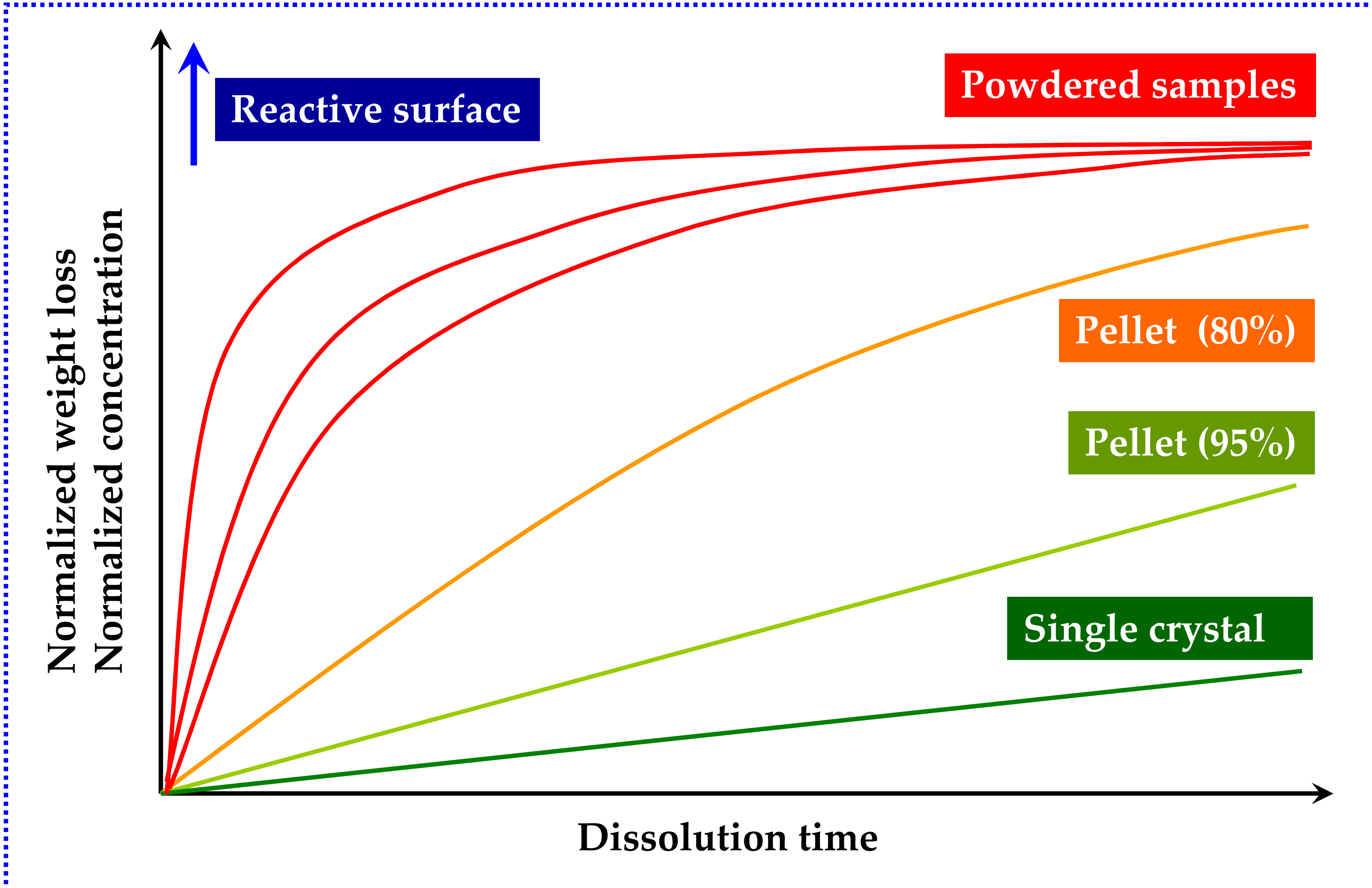

Open question :

Is there any role of the microstructure on the material dissolution ?

$$R_L = k_0 \times e^{-E_A/RT} \times a_{H+}^{\,n} \times g(I) \times \prod a_i^{mi} \times f(\Delta_R G)$$ × *f* (microstructure) ??

- Temperature contribution
- Acidity contribution
- Ionic strength contribution
- Redox, complexing contributions
- Deviation from thermodynamic equilibrium

Potential roles of

- Crystallization state ?
- Crystallite size ?
- Grain size ?
- Densification rate ?
- Heterogeneity ?
- … ?

Role of microstructural parameters

Crystallization state

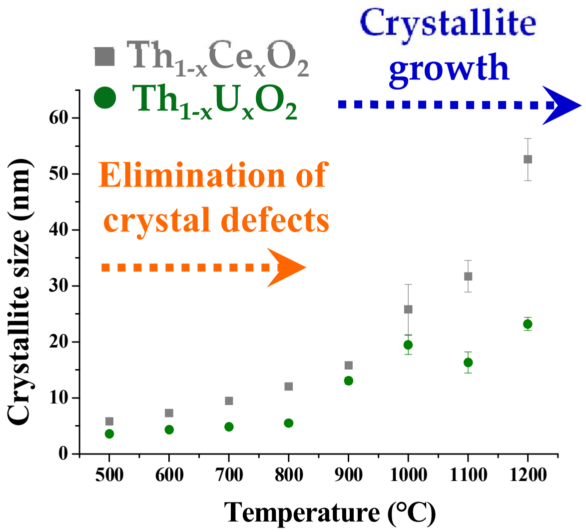

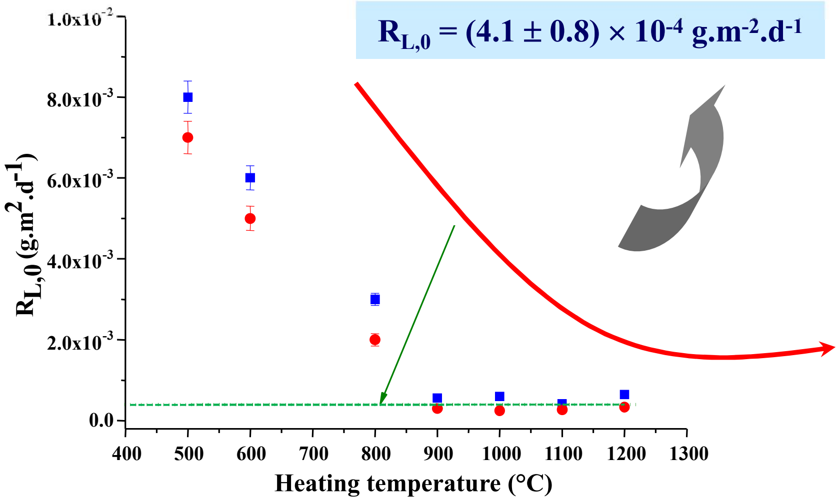

✦ Crystal defects : moderate impact ✦ Crystallite size : weak impact

Desnification rate

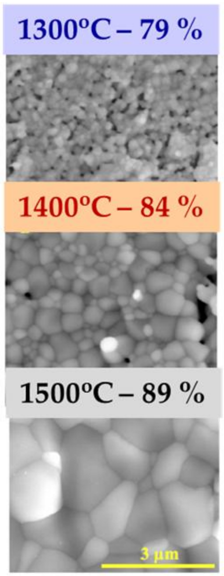

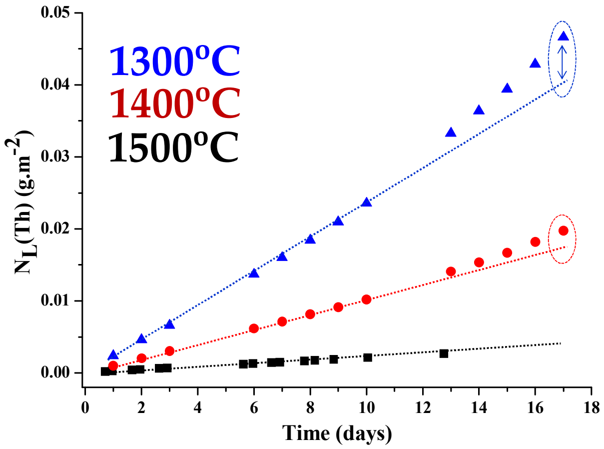

Densification & Grain size ↗
$R_{L,0}$ ↘ i.e. durability ↗

Cohesion & density of GB :
✦Moderate influence
✦Topological modifications

L. Claparede et al., Inorg. Chem., 50 (2011) 9059 & 50 (2011) 11702, J. Nucl. Mater., 457 (2015) 304

Microscopic study

Microstructural evolution of solid/solution interface

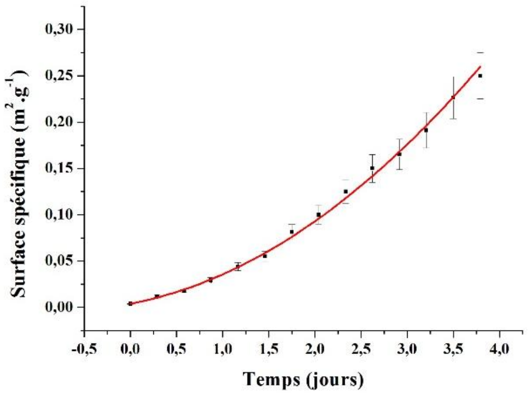

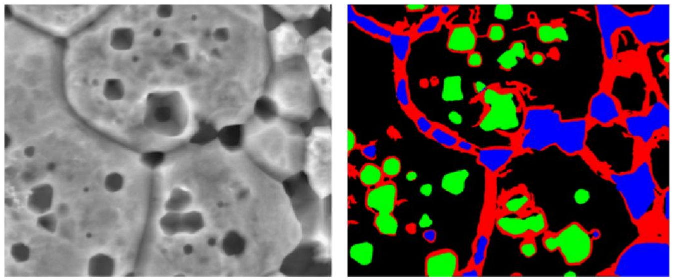

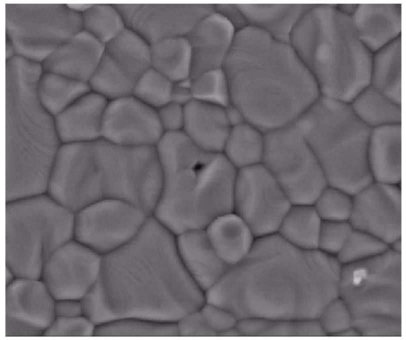

Operando study of evolving interface during dissolution

Dissolution tests

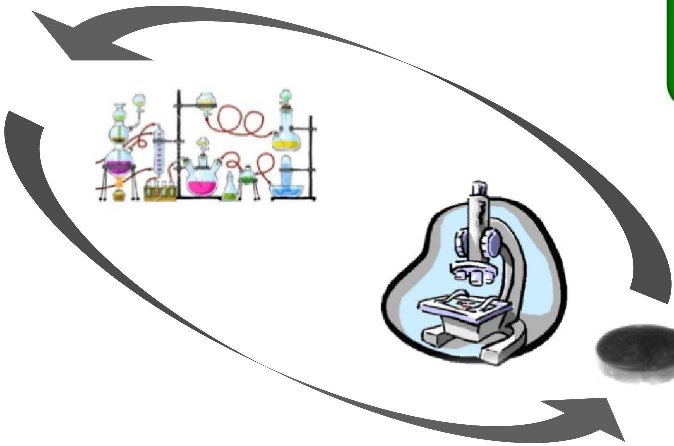

Environmental SEM observations

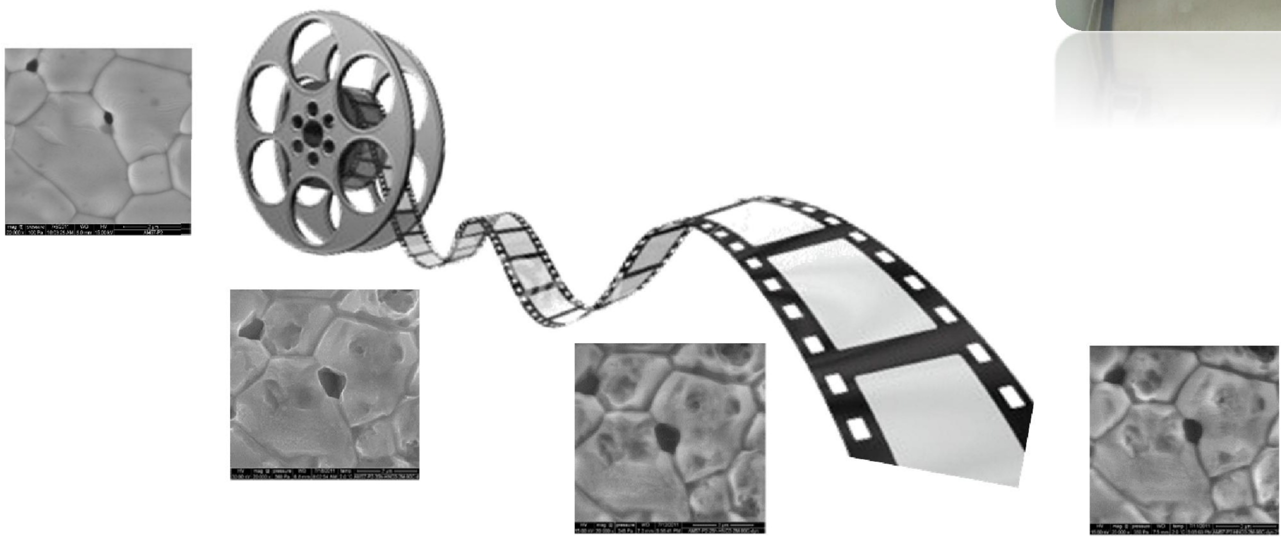

…

Operando study of $Th_{1-x}U_xO_2$ dissolution

$Th_{0.5}U_{0.5}O_2$ – 2M HNO_3 – T = 90°C

Grain boundarie

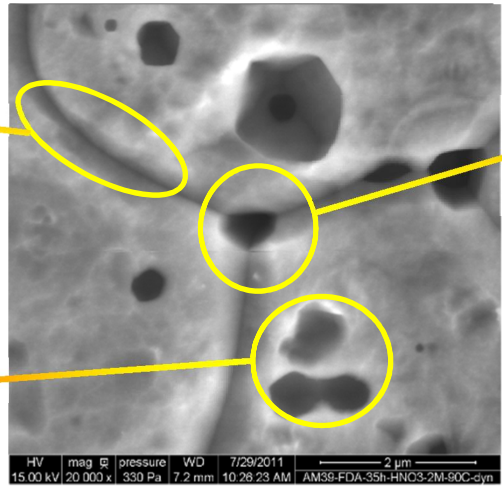

Triple junction

Corrosion pits

Strong microstructural evolution at solid/liquid interface

Main Open Questions

- ➢ Good evaluation of the initial reactive surface area ?
- ➢ What evolution of reactive surface area during dissolution ?
- ➢ What impact on the normalization ?
- ➢ What impact on the accuracy of the final obtained results ?

Some limitations

- ➢ Limited sample amounts
- ➢ Expected low S_{SA} values
- ➢ Impact of microstructure

~~Geometric determination~~

~~BET Analyses~~

Evaluation of Specific Surface Area (SSA) : SESAM method

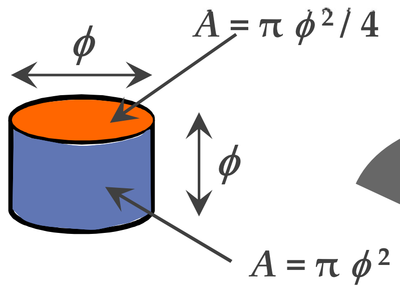

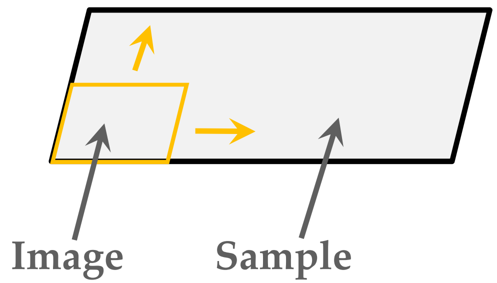

① Disc surface

② Integration on image surface

③ Integration on sample surface

④ Integration on sample volume

⑤ Correction by the open porosity ratio

Estimated specific surface area

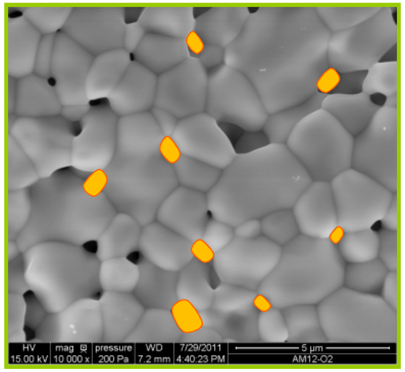

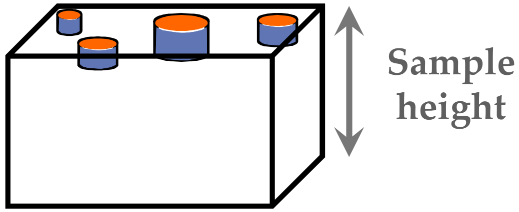

Grayscale threshold then binarization:

Surface area of the pores

Evaluation of SSA: SESAM method

Compound	Specific Surface Area ($m^2.g^{-1}$)		
	BET method (Kr)	*SESAM method*	*Geometrical*
CeO_2	0.180 (20 pellets , ≈ 5 g)	0.241	3.3×10^{-4}
UO_2 (reference)	< LoD	5×10^{-2}	2.6×10^{-4}
$Th_{0.5}U_{0.5}O_2$	< LoD	3×10^{-3}	2.6×10^{-4}
$Th_{0.25}U_{0.75}O_2$	< LoD	2×10^{-2}	2.6×10^{-4}
UO_2 + PGM	< LoD	2×10^{-2}	2.6×10^{-4}
$U_{0.9}Ln_{0.1}O_{1.95}$	1.5×10^{-2} (5 pellets , ≈ 1 g)	5×10^{-2}	2.9×10^{-4}

BET → SESAM: × 1.3 – 3.3

Geometrical → SESAM: × 77 - 730

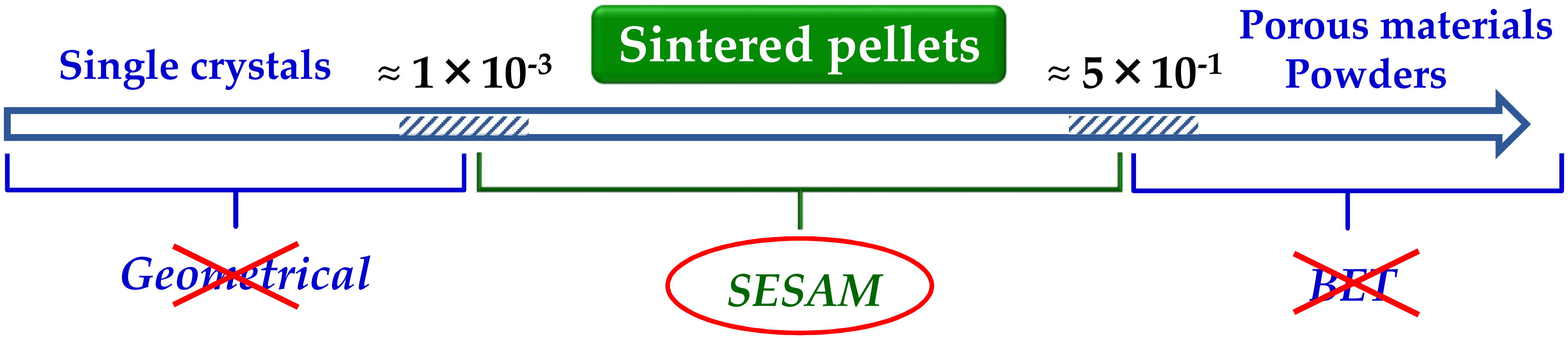

* *T. Cordara*, PhD, ICSM/CEA, Univ. Montpellier, Nov. 2017

Monitoring of solid/liquid interface during dissolution by ESEM

Monitoring of solid/liquid interface during dissolution by ESEM

$Th_{0.5}U_{0.5}O_2$ pellet
2M HNO_3 – T = 90°C
Time intervals : 7 hours

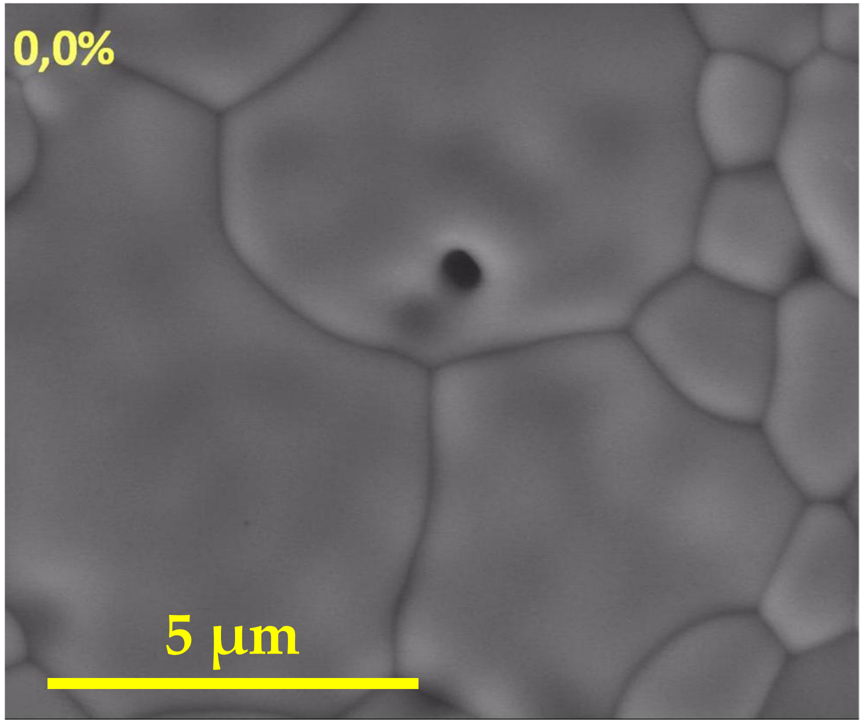

Heterogeneous dissolution

Preferential dissolution zones : GB, triple junctions, pores

Formation of corrosion pits

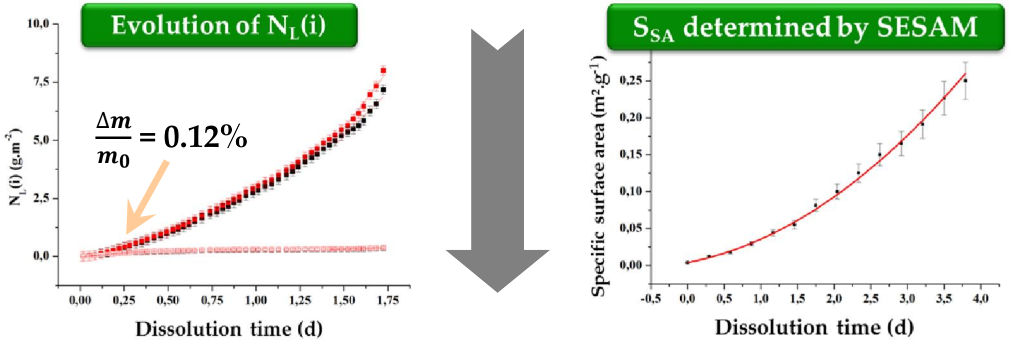

Surface reactions controlling dissolution

Correction of S rapidly required

$\Delta m/m_0 = 3\% \Leftrightarrow S/S_0 \approx 20$

Monitoring of solid/liquid interface during dissolution by ESEM

$Th_{0.25}U_{0.75}O_2$ pellet / 4M HNO_3 – RT

Time intervals : 1 hour

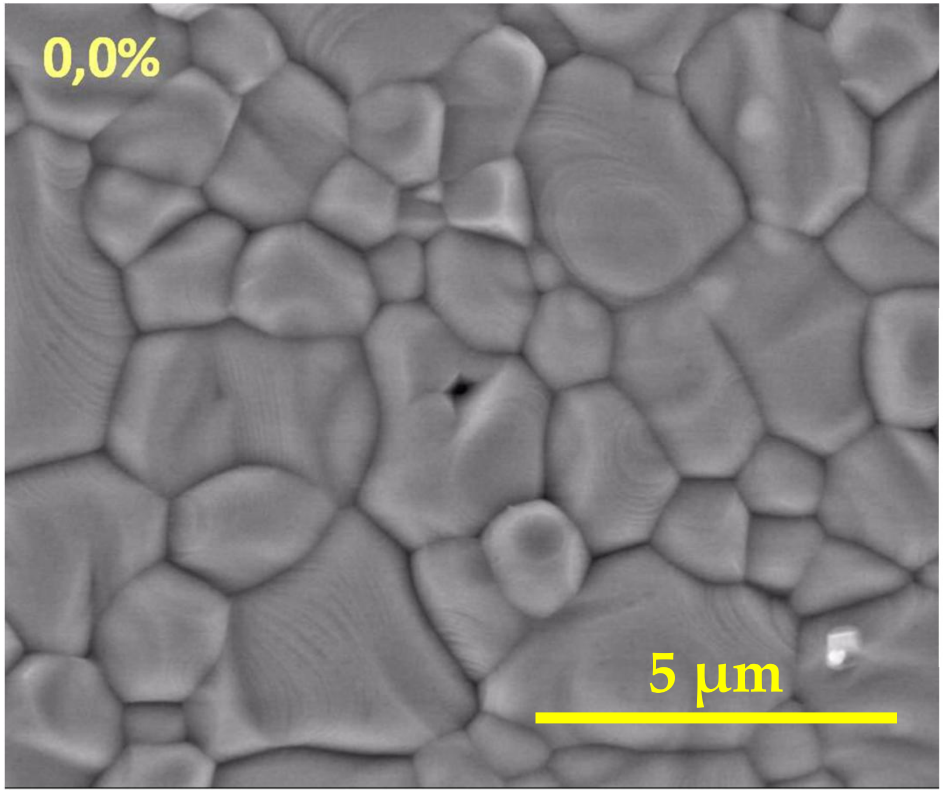

Homogenous dissolution

Degradation of the entire interface

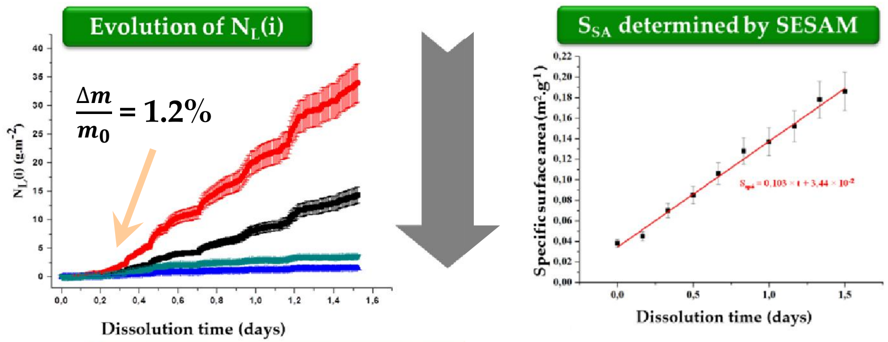

Redox reactions controlling dissolution

$\Delta m/m_0 = 22\% \Leftrightarrow S/S_0 \approx 5$

Monitoring of solid/liquid interface during dissolution by ESEM

UO_2 pellet
1 M HNO_3 – T = 60°C
Dissolution time : 3.2 days

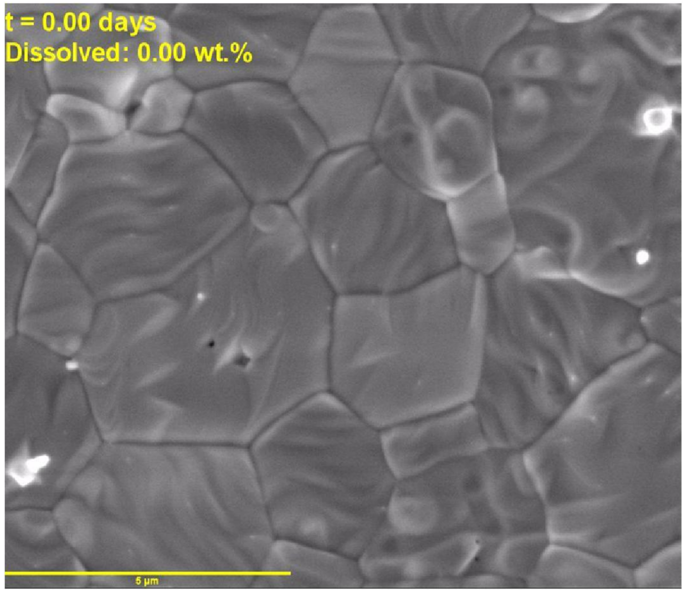

Homogeneous dissolution
Microstructural evolution
Oxidation of U(IV)

T. Cordara, PhD, ICSM/CEA, Univ. Montpellier, Nov 2017

$U_{1.9}Ln_{0.1}O_{1.95}$ pellet
1 M HNO_3 – T = 60°C
Dissolution time : 1.6 days

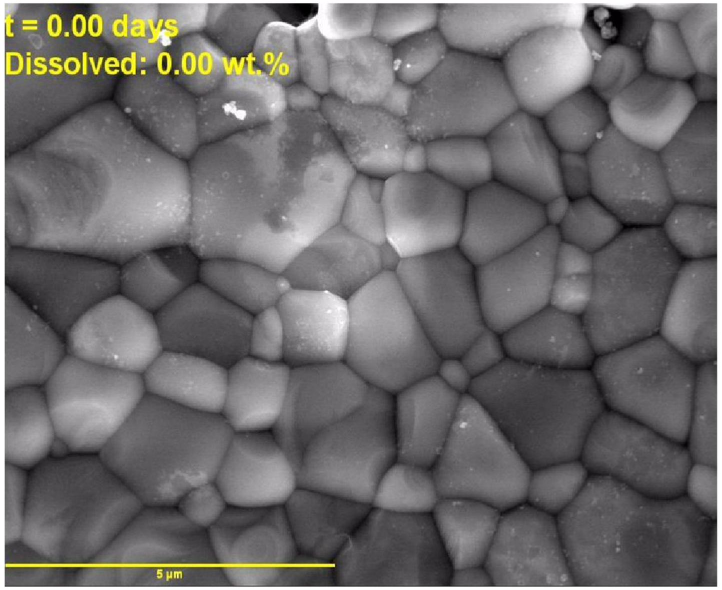

Preferential dissolution zones (GB)
Ln(III) – enrichment in GB
➯ Decrease of energy of cohesion

D. Horlait et al., J. Nucl. Mater., 2012, 429, 237
S. Szenknect et al., J. Phys. Chem. C 2012, 116, 12027

Impact of PGM : contribution at the solid/solution interface

UO_2 pellet with 3 mol.% PGM
0.1 M HNO_3 – T = 60°C
Dissolution time : 58 days

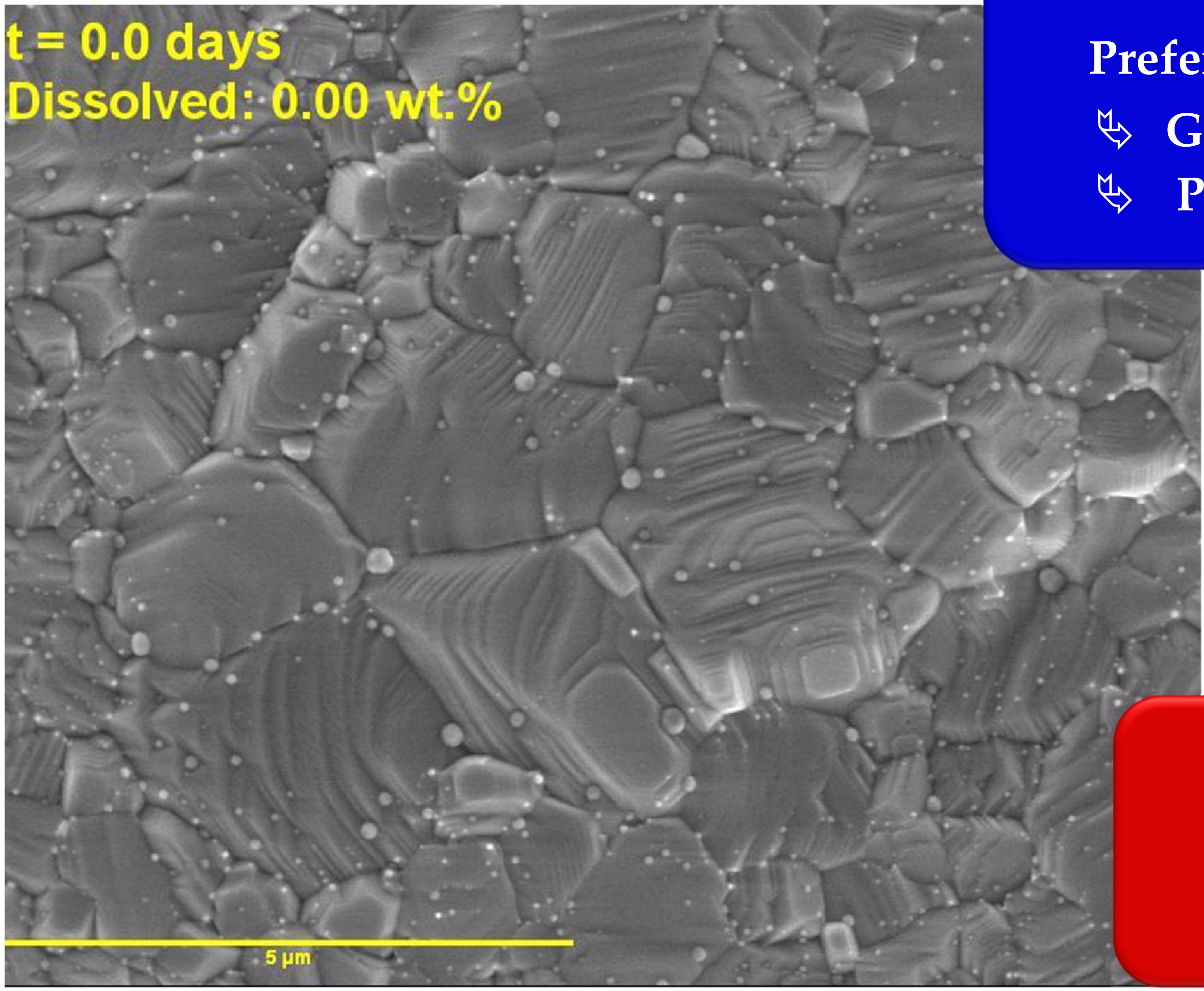

Heterogeneous dissolution

Preferential dissolution zones :

- GB, triple junctions, pores
- PGM / UO_2 / Solution interface

Evolution of $N_L(U)$

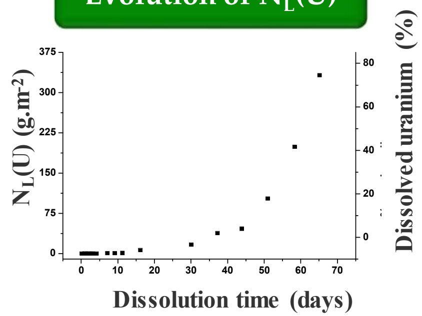

Surface reactions controlling dissolution

Impact of PGM @ Solid/Liquid interface

T. Cordara, PhD, ICSM/CEA, Univ. Montpellier, Nov 2017

3D analysis of the dissolution of UO_2 + PGM

Sintered UO_2 doped with 3 mol% Rh-Ru-Pd

0.1 M HNO_3 – 60°C

Operando ESEM:
Sequence of stereoscopic images

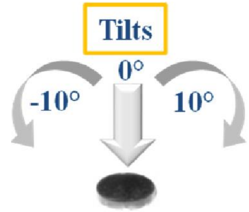

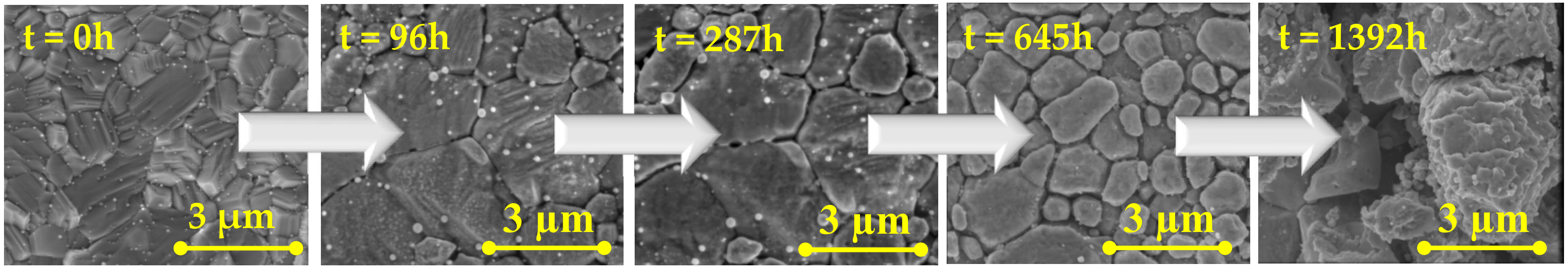

3D Reconstruction

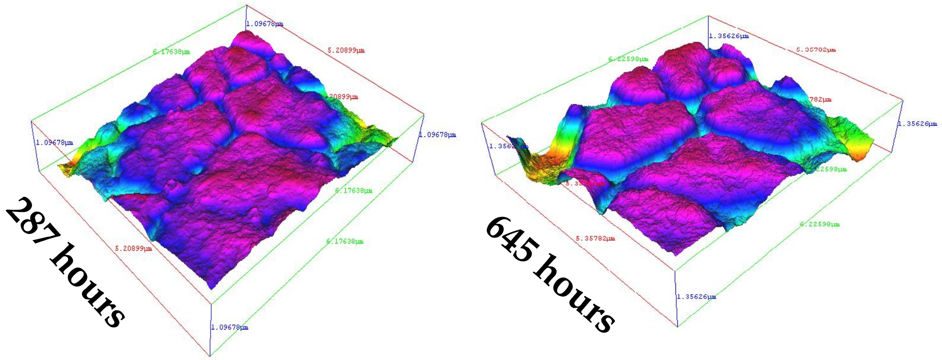

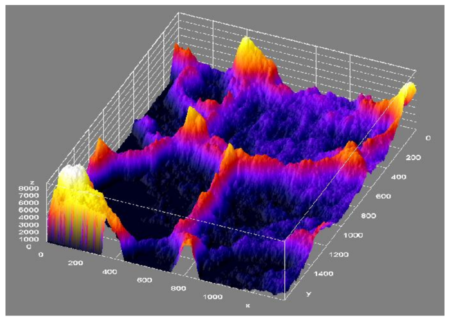

Zones of interest: Access to dissolved volumes

* *T. Cordara*, PhD, Univ. Montpellier, Nov. 2017

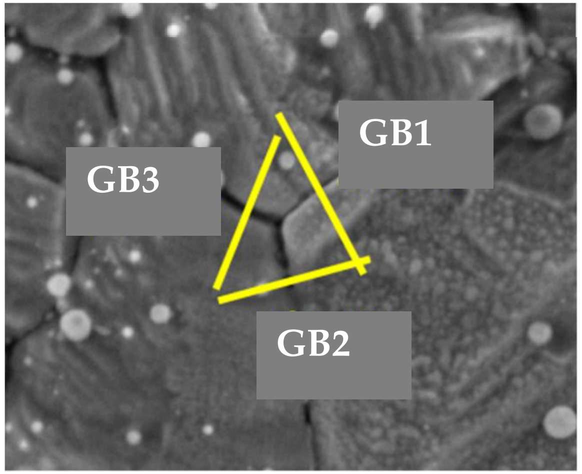

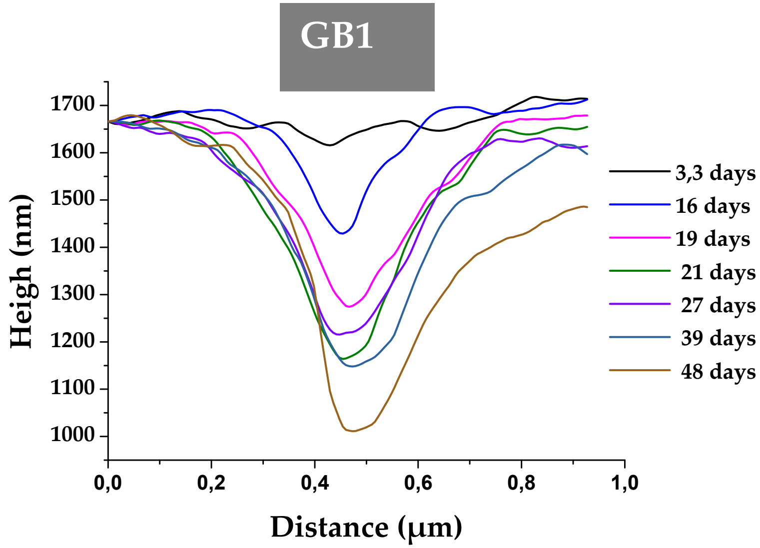

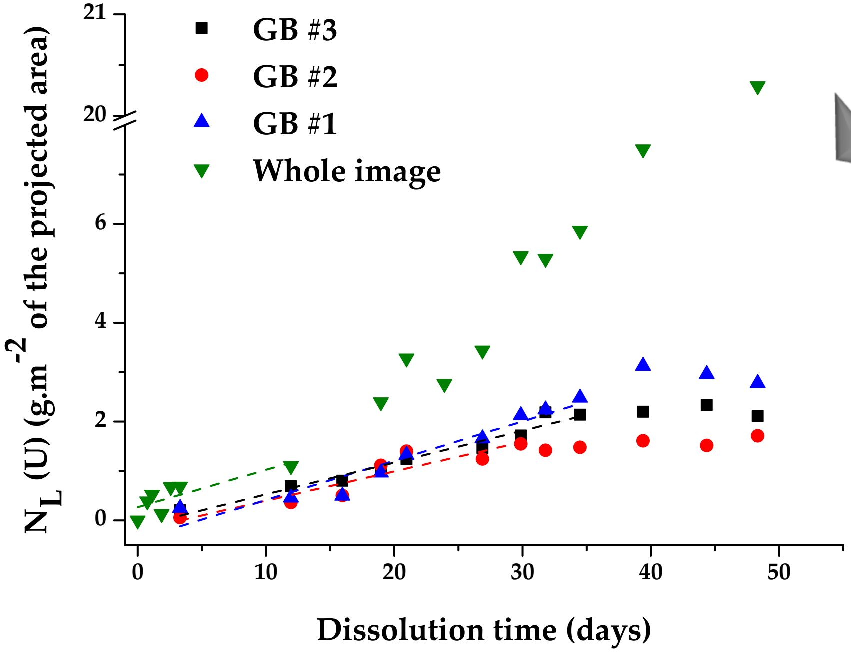

$R_{L,0}$ (global) = 7.4 × 10^{-2} g.m^{-2}.d^{-1}

$R_{L,0}$ (GB) = (6.5 to 8.4) × 10^{-2} g.m^{-2}.d^{-1}

Starting global dissolution directly linked to the dissolution of GB

Impact of the heterogeneity on the dissolution

Operando monitoring of surface composition

$Th_{0.5}U_{0.5}O_2$ – 2M HNO_3 – T = 90°C – Heterogeneous material

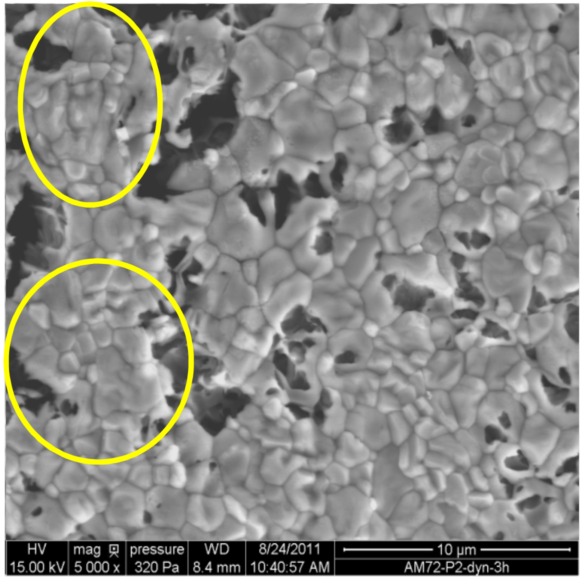

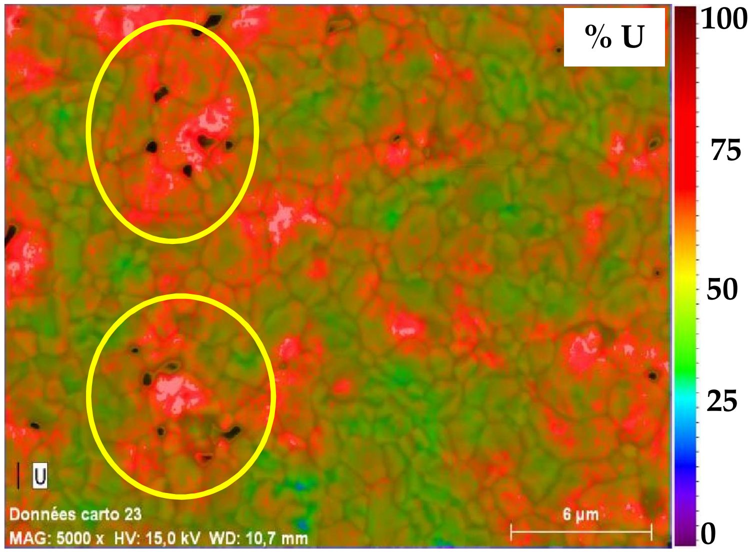

Preferential dissolution of U-enriched zones

Strong modifications of the surface composition

Strong impact on the reactive surface area

Impact of heterogeneity

$Th_{0.5}U_{0.5}O_2$ – Heterogeneous material – 2M HNO_3

Evolving composition : $f_i(t)$

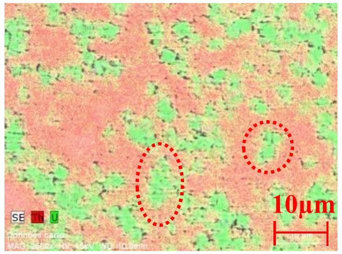

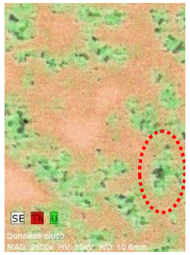

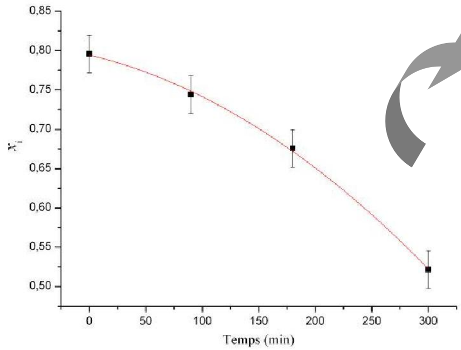

$f_i(t) = -1.9 \times 10^{-6}\ t^2 - 3.4 \times 10^{-4}\ t + 0.8$

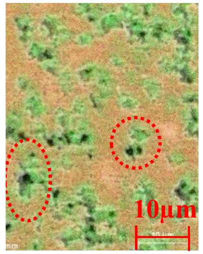

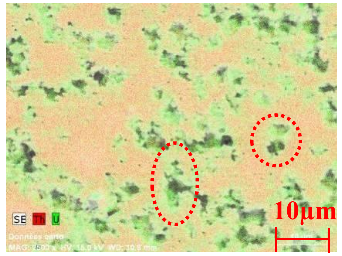

t = 0 min. t = 90 min. t = 180 min. t = 300 min.

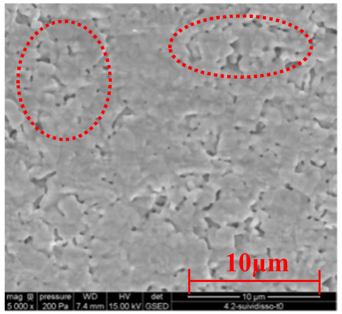

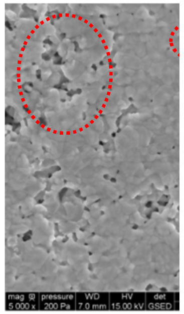

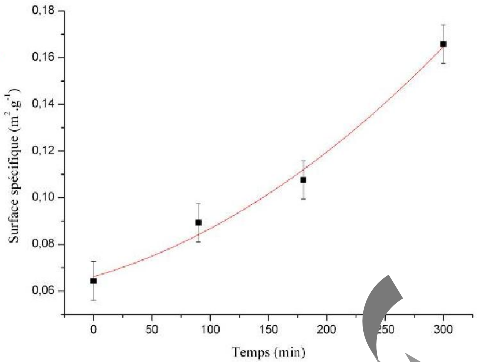

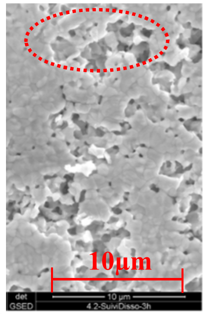

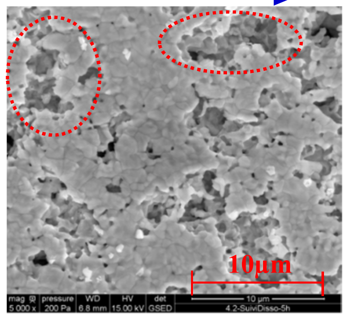

Evolving surface : S(t)

$S(t) = (6.1 \times 10^{-7}\ t^2 + 1.5 \times 10^{-4}\ t + 0.07)\ m(t)$

Macroscopic level incongruent dissolution (preferential U release) → **Image Analysis** → **Microscopic level congruent dissolution (U enriched zones)**

Main Conclusions & Overviews

Relative contribution of parameters during dissolution

$M_{1-x}Nd_xO_{2-x/2}$ & $Th_{1-x}U_xO_2$

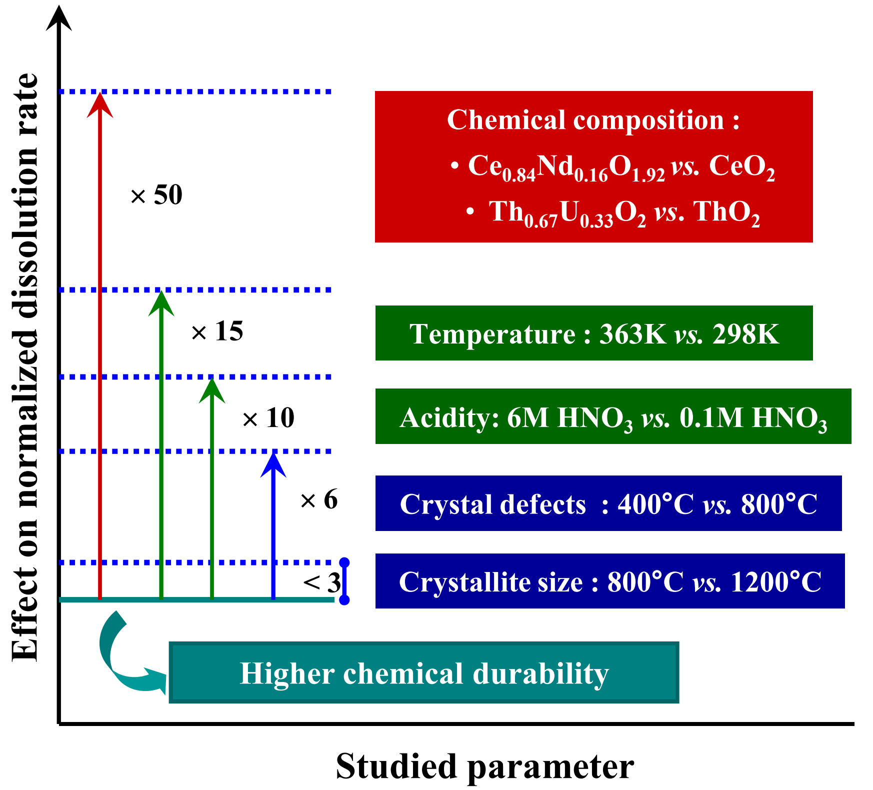

- Crystallization state
- Crystallite size / grain size
- Densification rate / GB density
- Heterogeneity (incl. surface)
- …

$$R_L = k_0 \text{ x } e^{-E_A/RT} \text{ x } a_{H+}^{\,n} \text{ x } g(I) \text{ x } \prod a_i^{mi} \text{ x } f(\Delta_R G)$$ × *f* (microstructure)

Examples of remaining open questions…

- **Discrimination of the impact of PGM's on the global dissolution process**
  - **Individual role of Ru, Rh, Pd (solubilized redox species)**
  - **Impact of the presence of secondary phases (i.e. perovskite for Mo)**
- **Precise impact of nitrogen based species coming from reduction of HNO_3**
  - **Combined effect (increase of production by PGM's)**
- **Particular behavior of $(U,Ce)O_2$ solid solutions**
  - **Impact of the "sample history" on the speciation of U and Ce**
  - **Consequence of redox reactions U(IV)/Ce(IV), U(V)/Ce(IV) @ the interface**
- **Impact of structural parameters**
  - **Effect of oriented MO_2 surface (single crystals) on the dissolution kinetics**
  - **Impact of dislocation loops at the interface**
- **Impact of porosity (confined volumes) on the development of reactions**
- **Impact of irradiation and irradiation/dissolution couplings**


Thank you for listening…

❖ Cristallites

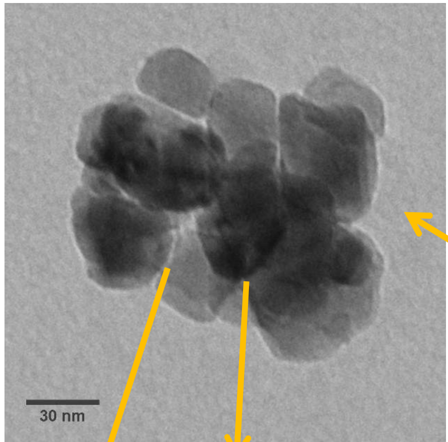

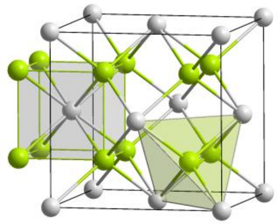

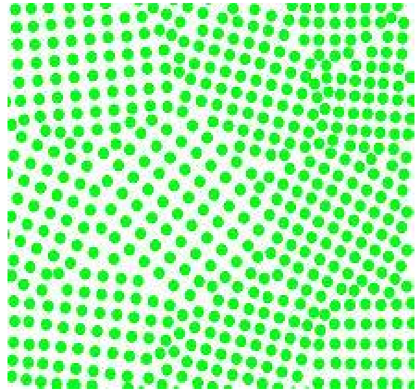

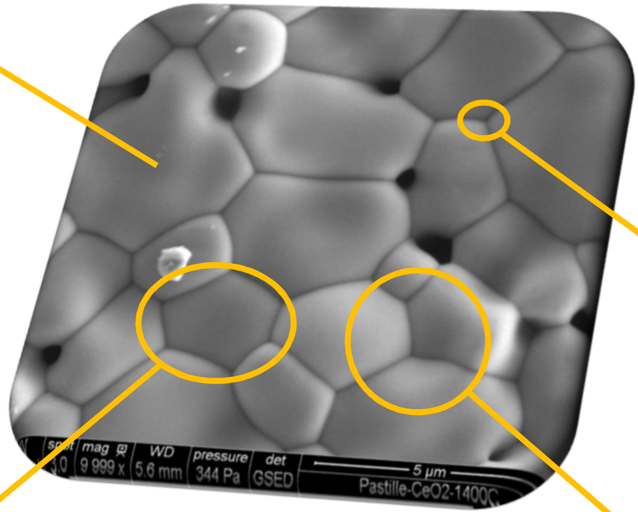

❖ Crystallite boundaries

❖ Triple junctions

❖ Grains

❖ Grain boundaries